

# Bias-corrected UKCP18 Convection-Permitting Model Projections for England

Qianyu Zha<sup>1</sup>, Yi He<sup>1</sup>, Timothy J. Osborn<sup>2</sup>, Nicole Forstehäusler<sup>1</sup>

<sup>1</sup>Tyndall Centre for Climate Change Research, School of Environmental Sciences, University of East Anglia, Norwich, NR4 7TJ, UK

<sup>2</sup>Climatic Research Unit, School of Environmental Sciences, University of East Anglia, Norwich, NR4 7TJ, UK

*Correspondence to:* Yi He (Yi.he@uea.ac.uk)

**Abstract.** The UKCP18 Convection-Permitting Model (CPM) provides the latest high-resolution climate projections for the UK. Compared with regional climate model projections, the CPM projections are more capable of simulating small-scale atmospheric convection particularly during extreme weather events such as intense rainfall and localised storms. However, systematic biases still exist in these projections. To improve the reliability of these projections, bias correction is crucial. In this study, we apply and evaluate a quantile mapping (QM) bias correction method for UKCP18-CPM hourly precipitation (with diurnal correction) and daily temperature over England. We quantify how closely the bias corrected simulations align with observations relative to the raw simulations. The raw UKCP18-CPM simulations exhibit wet precipitation biases, particularly in northern England, with annual mean biases ranging from 4.6% to 18.3%, and cool temperature biases, with annual mean biases from -0.87 °C to 0.02 °C. Bias correction substantially improved agreement with observational datasets, increasing  $R^2$  values for the 95<sup>th</sup> percentile of hourly precipitation from 0.80–0.88 to 0.98 and achieving near-perfect alignment ( $R^2 = 1$ ) for temperature extremes. Future projections for the 2070s indicate notable increases in annual maximum precipitation by 25.1–39.1% and mean daily temperature by 3.1 °C to 4.5 °C, highlighting the potential for more intense climate-related events. Overall, the applied bias-correction method brings UKCP18-CPM simulations into closer agreement with observations for both mean behaviour and extremes, providing a more reliable basis for high-resolution impact modelling and assessments that require hourly precipitation forcing.

## 1 Introduction

Global climate models (GCMs) are important tools for simulating present and future climates, widely used to project potential climate scenarios and assess the impacts of climate change on a global scale (IPCC, 2023a). However, GCMs often operate at relatively coarse spatial resolutions (ranging from 0.5° to 2.5°) and temporal scales (e.g., daily or monthly, seasonally, or annually), which can limit their ability to accurately represent fine-scale regional climate variations (IPCC, 2023b; Keller et al., 2022; Tabari et al., 2021). This underscores the need for higher-resolution climate data to improve regional impact assessments. To address this, regional climate models (RCMs) are commonly employed to dynamically downscale GCM outputs, generating data with finer spatial resolutions (typically between 0.1° and 0.5°). RCMs provide

several potential benefits over GCMs, such as the ability to better represent local topographical features, improve simulations of extreme weather events, and offer more refined regional climate projections, particularly in areas with complex terrain and climate variability (Chokkavarapu and Mandla, 2019; Kendon et al., 2010; Vichot-Llano et al., 2020). Convection-permitting models (CPMs) have become a valuable tool in short-range weather forecasting due to their enhanced ability to represent convective processes in detail, improve forecast accuracy, and capture localised high-impact rainfall that coarser models often miss (e.g., Done et al., 2004; Lean et al., 2008; Roberts and Lean, 2008; Weisman et al., 2008; Weusthoff et al., 2010). CPMs have also been widely applied in Europe (Berthou et al., 2020; Pichelli et al., 2021), Asia (Murata et al., 2017; Yun et al., 2020), and Africa (Kendon et al., 2019a; Maurer et al., 2017), as well as other regions (Trapp et al., 2011), to enhance the representation of convective processes and improve the accuracy of climate projections.

The UK Climate Projections 2018 (UKCP18) provide the latest generation of national climate projections for climate impact studies for the UK (Murphy et al., 2018). Several recent studies have employed the UKCP18-RCM 12 km regional perturbed parameter ensemble (PPE), which was released in November 2018, to assess the potential impacts of climate change. These applications include investigations into river and groundwater flow (Hannaford et al., 2023; Kay et al., 2023), extreme weather events (Hanlon et al., 2021), flood risks (Gudde et al., 2024), and droughts (Reyniers et al., 2023). In 2019, an additional UKCP18 toolkit was introduced, featuring the 2.2 km Convection-Permitting Model (UKCP18-CPM), which offers access to reliable climate information at local and hourly scales (Kendon et al., 2019b).

Despite their widespread use, climate model projections often show systematic biases relative to observations (Kotlarski et al., 2014; Vautard et al., 2021). For example, the UKCP18-RCM 12 km ensemble shows biases, including overestimation of winter precipitation, particularly in the mean and the 95th percentile of daily precipitation (representing heavy precipitation events) across most regions, and strong spatial variability in summer, with overestimations in the north and underestimations in the south (Reyniers et al., 2025). For temperature, the ensemble shows an overall cold bias at the annual scale in the mean and extremes. In winter, biases vary spatially and suggest overestimated variability, whereas in summer temperatures are more consistently underestimated across the UK (Reyniers et al., 2025). Building on the UKCP18-RCM, the UKCP18-CPM offers improvements, though notable issues persist. In winter, it remains too wet across most of the UK, while in summer it is too wet in the north and too dry in the south (Kendon et al., 2021). For temperature, the UKCP18-CPM slightly reduces UK-wide biases in summer compared to the UKCP18-RCM, although it remains cooler in the far north and exhibits minimal differences elsewhere (Kendon et al., 2021). In winter, the UKCP18-CPM introduces colder biases, particularly in northern regions, which are linked to its improved representation of snow processes, leading to greater snow accumulation and cooler temperatures (Kendon et al., 2021).

These biases, if left uncorrected, can severely affect the accuracy of climate impact assessments in sectors such as hydrology, ecology, and agriculture. The non-linear responses of impact models to these biases can amplify errors in projections, underscoring the importance of applying bias correction (BC) before using climate data in impact studies. In this paper, we use the term bias correction (BC) following common usage in the climate impact literature. However, these methods do not remove model biases in a physical sense; rather, they statistically adjust model outputs to better match an observational

65 reference over a calibration period. We adopt this interpretation when discussing our results. Various BC methods, such as  
statistical downscaling, linear scaling, local intensity scaling, histogram equalizing, rank matching, and quantile mapping  
(QM), have been developed and evaluated (Gutmann et al., 2014; Maraun et al., 2019; Teutschbein and Seibert, 2012).  
Amongst these, QM has emerged as a particularly effective approach (Lafon et al., 2013; Shah et al., 2024; Themeßl et al.,  
70 and precipitation adjustments in climate impact studies (Fang et al., 2015; Themeßl et al., 2012; Wilcke et al., 2013). For  
example, Cannon et al. (2015) evaluated the QM for bias correction of GCM precipitation outputs, emphasizing its  
effectiveness in adjusting mean values and precipitation extremes, while Sangelantoni et al. (2019) demonstrated its  
applicability for RCM temperature and precipitation corrections over Central Italy, particularly for seasonal and extreme  
climate variables.

75 In the UK, the UKCP18-RCM ensemble dataset has been widely used and bias-corrected for applications such as river flow,  
flood risk, and drought assessments (Hannaford et al., 2023; Robinson et al., 2023; Smith et al., 2025). In contrast, bias  
correction of the UKCP18-CPM ensemble remains limited. Kay and Brown (2023) applied a simple monthly scaling method  
to correct daily UKCP18-CPM precipitation data from the ensemble member 01 (EM01) against observations and kept  
temperature data uncorrected. However, this monthly scaling applied a uniform adjustment to all daily precipitation values  
80 within each month. It corrects monthly means but does not explicitly adjust the within-month distribution (e.g., quantiles and  
extremes). As a result, it may not accurately correct biases in extreme precipitation events. It also fails to correct the diurnal  
cycle of precipitation, which is a key feature of high-resolution climate models (Bannister et al., 2019; Scaff et al., 2019).  
This is consistent with Faghieh et al. (2022), who compared two bias-corrected time series using a multivariate quantile  
mapping method, both with and without correction of the diurnal cycle, and found that bias correction of the diurnal cycle  
85 for sub-daily precipitation is preferable. Moreover, bias correction of sub-daily variables from CPMs is rare, largely due to  
two main challenges: (1) the substantial computational and memory demands associated with processing sub-daily data from  
high-resolution climate models, and (2) the relative scarcity of hourly observational datasets compared to daily observations,  
which poses challenges for the evaluation and correction of sub-daily variables from CPMs.

This study leverages a 1 km resolution gridded hourly observation-based rainfall dataset (CEH-GEAR1hr) for bias  
90 correcting the UKCP18-CPM hourly precipitation data. The CEH-GEAR1hr dataset (Lewis et al., 2022) integrates data from  
over 1,900 quality-controlled rainfall gauges over Great Britain, providing highly accurate precipitation measurements and  
enabling more robust sub-daily evaluation and bias correction of precipitation timing and intensity. For temperature, there is  
currently no observation-based hourly temperature dataset across the UK. Therefore, bias correction was performed on the  
UKCP18-CPM daily temperature using the Met Office's 1 km daily HadUK-Grid dataset (Hollis et al., 2019; Met Office et  
95 al., 2022). Building on the findings of Faghieh et al. (2022), we address a remaining gap: diurnal-cycle-aware bias correction  
is still rarely implemented and systematically evaluated for sub-daily precipitation in convection-permitting climate  
simulations, despite its importance for impact models that are sensitive to rainfall timing and intensity. The contribution of  
this paper is therefore application-driven evaluation in a CPM sub-daily setting, providing evidence on whether

incorporating diurnal structure within quantile mapping improves (i) conventional climatological statistics and (ii) more  
100 challenging characteristics, including the diurnal cycle and sub-daily extremes.

The purpose of this paper is to present and assess a bias-correction method for UKCP18-CPM hourly precipitation and to  
quantify how closely the bias-adjusted UKCP18-CPM simulations align with observations relative to the raw simulations.  
We bias-corrected and evaluated the hourly precipitation and daily temperature variables from the UKCP18-CPM for  
England using the quantile mapping (QM) method. The UKCP18-CPM (Kendon et al., 2019b) consists of a 12-member  
105 convection-permitting model ensemble, which is nested within a 12-member RCM perturbed parameter ensemble (PPE), and  
further nested within a 12-member GCM PPE. Due to storage and computational constraints, we referenced the CHES-  
SCAPE dataset (Robinson et al., 2023) and selected four ensemble members for this study (Sect. 2.3.1 Choice of sub-  
ensemble), including the default configuration EM01 (also the driest member), the wettest members (EM04 and EM07), and  
a moderate member (EM08). The bias-corrected dataset features a high spatial resolution of 1 km, with hourly precipitation  
110 and daily temperature data. Specifically, we address the following research questions:

1. What biases are contained in the UKCP18-CPM simulations?
2. Can the QM bias correction method successfully correct errors in simple and more challenging metrics?
3. What climatic changes do the UKCP18-CPM ensemble members broadly project for England?

Addressing these questions is crucial for understanding and improving the applicability of UKCP18-CPM data in climate  
115 impact assessments.

## 2 Study area, data and methods

### 2.1 Study area

This study focuses on England (Fig. 1), with the primary aim of assessing the bias-correction method. Catchment boundaries  
are obtained from 249 catchments in the National River Flow Archive (NRFA) and are used only to define the analysis mask  
120 (i.e., to select the 1 km grid cells processed). Appendix A. Table A1 lists the NRFA IDs of the 249 catchments used to define  
the analysis mask in this study. No hydrological modelling or catchment-scale simulation is performed. The processed  
HadUK-Grid cells within this mask are displayed in Fig. 1 by their centre points. Given computational and storage  
constraints, restricting the analysis to grid cells within these catchments provides a practical and geographically coherent  
subset for the study. The catchments were selected based on the availability of complete gauged records for December 1990  
125 to November 2000, overlapping with both the CEH-GEAR1hr observational dataset and the UKCP18-CPM baseline period  
(see Sect. 2.2.2; hereafter referred to as the reference period), and on minimal anthropogenic influence. Bias correction was  
applied independently at the grid-cell level to UKCP18-CPM precipitation and temperature for 62,488 1 km grid cells.  
Across the processed grid cells, the mean annual precipitation is approximately 2.64 mm d<sup>-1</sup>, and the mean annual  
temperature is around 9.3 °C, based on the CEH-GEAR1hr and HadUK-Grid datasets, respectively.

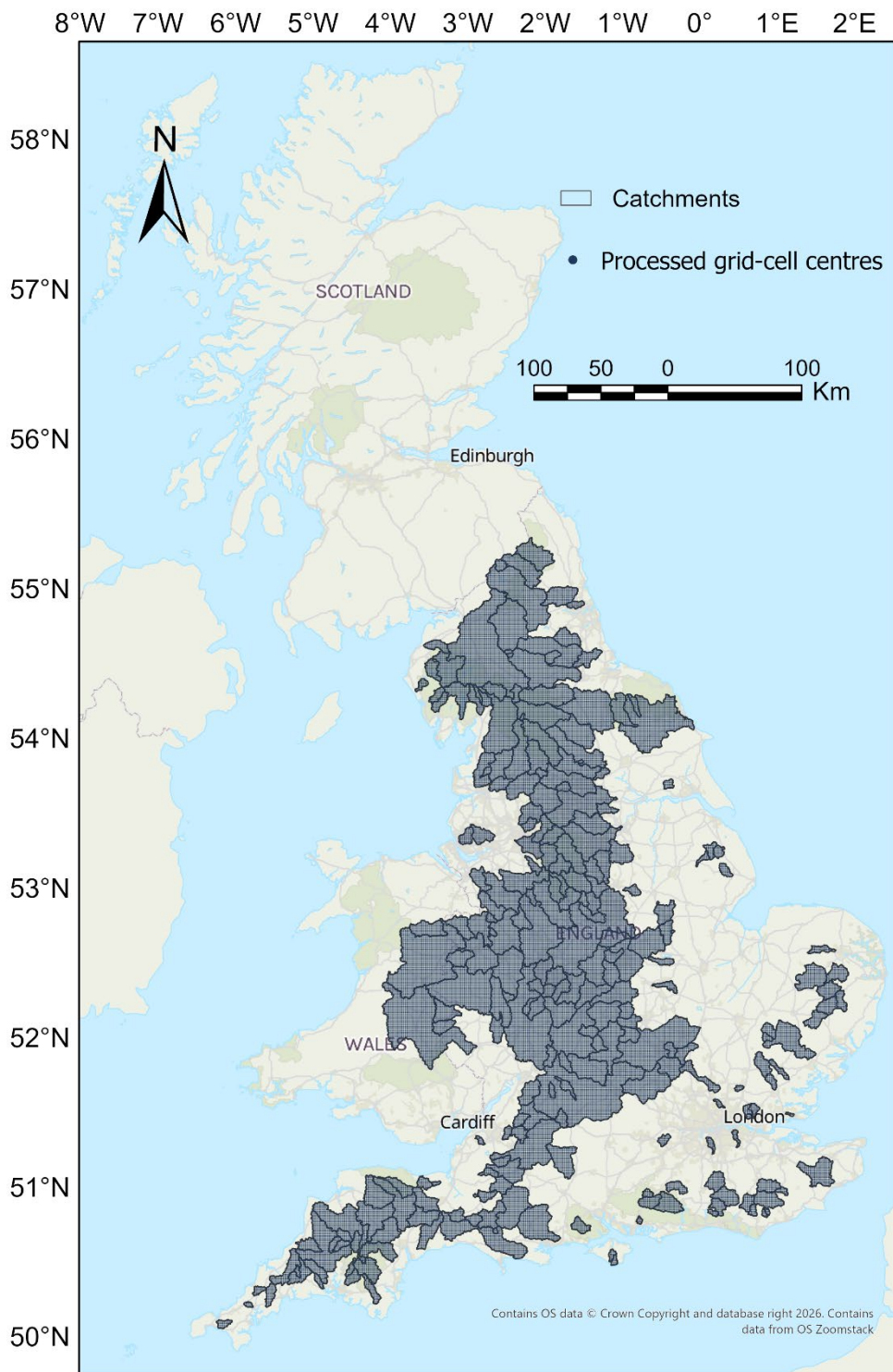


**Figure 1 Study domain in England. Catchment boundaries (249 catchments) are used only to define the analysis mask for grid-cell processing. The processed 1 km HadUK-Grid cells are displayed by their centre points.**

## 2.2 Datasets

### 135 2.2.1 UKCP18 Convection-permitting model projections (UKCP18-CPM)

The UK Climate Projections 2018 (UKCP18) represent the latest set of national climate projections for the UK, offering a broad range of temporal coverage and spatial resolutions (Murphy et al., 2018). The land component of UKCP18 comprises three strands of information. Strand 1 updates the probabilistic predictions from UKCP09, providing a more comprehensive range of possible climate outcomes under specified emission scenarios. Strand 2 delivers a new set of global climate model (GCM) projections at approximately 60 km resolution, and it captures uncertainties in large-scale climate processes. Strand 3 is a perturbed parameter ensemble (PPE) of 12 regional climate model (RCM) projections derived from 12 of the 15 GC3.05-PPE simulations (Murphy et al., 2018). The projections from Strands 1, 2, and the 12 km RCM from Strand 3 were initially released in November 2018 (Murphy et al., 2018).

The UKCP18 convection-permitting model (UKCP18-CPM) projections are the UKCP18 Local (2.2 km) product (Kendon et al., 2019b), providing high-resolution climate information at ~2.2 km resolution and driven by the UKCP18 Regional (12 km) Strand 3 ensemble. These projections explicitly capture small-scale physical processes and extreme weather events that are inadequately represented at coarser resolutions. CPM data are available on their native ~2.2 km rotated lat-lon grid and re-projected to a 5 km grid aligned with the Great Britain national grid (Met Office Hadley Centre, 2019). This study uses the re-projected 5 km CPM data for ensemble members 01 (EM01), 04 (EM04), 07 (EM07), and 08 (EM08) (see details in Sect. 2.3.1 Choice of sub-ensemble). These ensemble members adopt the standard RCM parameterizations (note that CPM-specific parameters are not adjusted between ensemble members). The 5 km dataset (Met Office Hadley Centre, 2019) was further re-gridded to the 1 km grid using the nearest neighbour interpolation method, assigning each 1 km grid cell the value of the corresponding 5 km grid cell in which it is located. This method was chosen to preserve the original value distribution and avoid artificial smoothing or interpolation artefacts that could arise from bilinear or higher-order methods, which is particularly important for preserving extreme values in precipitation and temperature relevant to impact studies. At the time of this study, the UKCP18-CPM data was available in three 20-year time slices: 1980-2000 (December 1980 to November 2000; baseline period), 2020-2040 (December 2020 to November 2040; 2030s), and 2060-2080 (December 2060 to November 2080; 2070s). The latter two are based on the high emissions scenario RCP8.5, which assumes high population growth and energy demand (Riahi et al., 2011). The data has 360 days for each meteorological year that begins on 1<sup>st</sup> December and ends on 30<sup>th</sup> November.

## 2.2.2 Observation-based datasets

As an observational reference for the evaluation and bias correction of UKCP18-CPM hourly precipitation, we used the 1 km resolution gridded hourly observation-based rainfall dataset, CEH-GEAR1hr (Lewis et al., 2022). This dataset is derived through the application of the nearest neighbour interpolation method to a national database of hourly rain gauge observations. The initial version of this dataset was published in 2019, covering the period from 1990 to 2014, and subsequently updated in 2022 (CEH-GEAR1hr v2) to extend the coverage to 1990-2016 (Hollis et al., 2019). For this study, we used CEH-GEAR1hr v2, which is available at the UKCEH Environmental Information Data Centre (Lewis et al., 2022). To evaluate the bias in the raw UKCP18-CPM projections compared to observations, we selected the overlapping portion of data from December 1990 to November 2000 (reference period).

To the best of our knowledge, there is currently no gridded, observation-based dataset in the UK that provides nationwide hourly temperature at high spatial resolution. Additionally, uncertainties exist when disaggregating temperature variables from daily to sub-daily scales, as indicated by previous studies on meteorological disaggregation processes (Breinl and Di Baldassarre, 2019). Therefore, this study focuses on the bias correction of the UKCP18-CPM daily temperature. For reference, the HadUK-Grid dataset (Hollis et al., 2019) is used. This dataset comprises gridded climate variables derived from the network of UK land surface observations and is produced by the Met Office Hadley Centre. It interpolates in situ observations to a regular grid, following methods developed in earlier datasets made available through the UK Climate Projections project (UKCIP02, UKCP09). The study uses Version 1.1.0.0 of the dataset, available on the CEDA Archive (Met Office et al., 2022).

## 2.3 Methods

### 2.3.1 Choice of sub-ensemble

As described in Sect. 2.2.1 UKCP18 Convection-permitting model projections (UKCP18-CPM), UKCP18 Strand 3 introduces a new ensemble consisting of 12 RCM simulations, which form a PPE of RCM variants derived from 12 out of the 15 GC3.05-PPE simulations (Murphy et al., 2018). Ensemble member 01 (EM01) serves as the standard configuration, generated without any parameter perturbations to provide a baseline reference for the ensemble. The other members are produced by varying specific parameters, such as cloud microphysics, aerosol forcing, ocean heat uptake, and atmospheric processes, to assess the model's response under diverse conditions (Sexton et al., 2021).

The UKCP18-CPM consists of 12 projections driven by the 12 km RCM ensemble. Due to computational and storage constraints, it was not practical to bias-correct the full CPM-PPE at 1 km hourly resolution. We therefore selected a subset of ensemble members for bias correction and implemented a parallel workflow on the University of East Anglia's high-performance computing (HPC) system to complete the processing within a reasonable time. Four ensemble members were selected to represent the broad range of possible precipitation outcomes within the ensemble. This selection included the default configuration (EM01), as well as members representing the driest, wettest, and a more moderate response, focusing

on variability in precipitation. It is reasonable to assume the CPM members inherit the larger scale patterns and projected changes from their parent RCMs members due to the one-way nesting approach applied within UKCP18. Therefore, we referred to the future precipitation changes projected by the UKCP18-RCM ensemble to guide the selection of CPM ensemble members. Table 1 summarises the percentage changes of precipitation in the 12 UKCP18-RCM ensemble members for the period 2060-2080 relative to 1980-2000.

**Table 1. Percentage changes of precipitation in the 12 UKCP18-RCM ensemble members between the 1980-2000 and 2060-2080 (Robinson et al., 2023).**

Ensemble member	Precipitation (%)				
	Annual	DJF	MAM	JJA	SON
01	-7	8	-2	-21	-17
04	5	21	4	-14	3
05	-2	8	1	-18	-4
06	-3	11	11	-40	-6
07	5	20	14	-27	5
08	1	15	9	-32	1
09	3	29	10	-33	-5
10	-2	13	7	-26	-8
11	-2	15	-5	-25	2
12	-3	13	-8	-17	-10
13	-5	23	-15	-38	-6
15	1	14	2	-25	4

\*Ensemble members used for this study

We chose the following:

- **EM01** represents the default parameterisation of the climate model, chosen as a reference point. EM01 is the driest member, showing an overall decrease in annual precipitation, characterised by the smallest increase in winter (DJF) precipitation and the largest reduction in autumn (SON) precipitation. It has the largest decrease in annual precipitation, making it a suitable choice for representing scenarios with very dry conditions.
- **EM04** exhibits the largest increase in annual precipitation, with substantial growth during winter (DJF), alongside smaller increases in spring (MAM) and autumn (SON), and the smallest reduction in summer (JJA). It represents the upper limit of precipitation increase, which is crucial for assessing wet scenario impacts.
- **EM07** is similar to EM04 in terms of annual precipitation increase but with a different seasonal distribution. EM07 shows pronounced increases in spring (MAM) and autumn (SON) but a greater decrease in summer (JJA). It is thus used to represent a scenario with more extreme seasonal variability.

- **EM08** represents a moderate change in annual precipitation, lying near the middle range of all 12 ensemble members. It shows limited change in autumn (SON) precipitation, various increases in winter (DJF) and spring (MAM), and a moderate decrease in summer (JJA). This makes EM08 an appropriate choice to illustrate balanced seasonal changes.

215

These four ensemble members were selected to capture a wide range of precipitation responses, from the driest to the wettest scenarios. This approach ensures that the corrected dataset captures a wide spectrum of possible outcomes, offering a robust understanding of potential precipitation changes across different seasons. The ensemble mean presented in this study represents the mean of these four selected members.

### 220 2.3.2 Bias correction

Quantile Mapping (QM) is a widely used bias correction method designed to address systematic discrepancies (biases) in climate model outputs by aligning their distributions with observed data, thereby enhancing the reliability of regional impact assessments (Ayugi et al., 2020; Ngai et al., 2017; Reyniers et al., 2025; Tani and Gobiet, 2019). The QM method applies a statistical transformation to correct modelled values based on observed distributions. This transformation can be expressed as

225 (Piani et al., 2010):

$$x^o = f(x^m) \quad (1)$$

Where  $x^o$  and  $x^m$  are the observed and modelled values, respectively, and  $f()$  is the transformation function. In practice, the transformation is achieved by aligning the cumulative distribution functions (CDFs) of modelled and observed data. It can be defined as:

$$x^o = F_{obs}^{-1}(F_{mod}(x^m)) \quad (2)$$

230 Where  $F_{mod}$  is CDF of the modelled value and  $F_{obs}^{-1}$  is the inverse of the observed CDF, also referred to as the quantile function. Therefore, QM effectively adjusts the CDFs of modelled climate variables to match the observed, thereby correcting not only the mean but also the variance and extreme values in the data (Cannon et al., 2015; Thrasher et al., 2012). Among the different variants of QM, the non-parametric variant, often referred to as empirical QM, adjusts modelled values using the empirical CDFs of the observed and modelled values, rather than assuming specific parametric distributions (e.g. Boé et al., 2007; Themeßl et al., 2011, 2012). The empirical CDFs are estimated using tables of empirical percentiles, with

235 linear interpolation applied to approximate values falling between the percentiles (Boé et al., 2007). This makes empirical QM particularly suitable for handling variables like temperature and precipitation, which frequently exhibit non-linear and heterogeneous behaviours (Gudmundsson et al., 2012). In this study, the empirical CDFs for observations and raw CPM are constructed using the baseline period, and the resulting mapping function is applied to the full CPM time series (3 20-year time slices).

240 As Reiter et al. (2018) pointed out, when applied to the full calibration period as a whole, QM can correct the overall distribution, but it does not correct errors in the annual cycle. They reviewed different subsampling lengths for quantile

mapping applications and found that subsampling improves the performance of bias correction for daily precipitation from climate models, with monthly timescales being optimal across all QM methods. Therefore, we applied empirical QM for both precipitation and temperature using monthly subsampling. For daily temperature, the data was first divided into 12 groups, one for each month, and empirical quantile mapping was applied to each group individually. For hourly precipitation, a single correction applied to all hours can miss the diurnal cycle. This may influence the reliability of climate model outputs, particularly in regional impact assessments involving small catchments that exhibit rapid hydrological responses to precipitation (Ban et al., 2014; Dai et al., 1999). To account for temporal variability, we applied a diurnal quantile mapping (DBC) method for hourly precipitation, based on Faghieh et al. (2022). The data for each month was further divided into 24 hourly groups, with a 3 h moving window used to compute the hourly data. This resulted in 24 unique correction factors, one for each hour of the day, to account for diurnal variability. Empirical QM was then applied to each hourly group. This approach enhances the representation of the diurnal cycle and improves the accuracy of bias correction for sub-daily precipitation. The QM method was implemented using the 'fitQmapQUANT' function from the qmap R package (version 1.0-4), developed by Lukas Gudmundsson (Gudmundsson et al., 2012). Key parameters were configured to enhance the accuracy of the correction: the argument 'qstep' was set to 100, following the findings of Lafon et al. (2013), who demonstrated that increasing the number of quantiles reduces errors, with 100 quantiles achieving optimal results. Additionally, 'type' was set to linear to specify the type of interpolation between quantiles.

### 3 Results

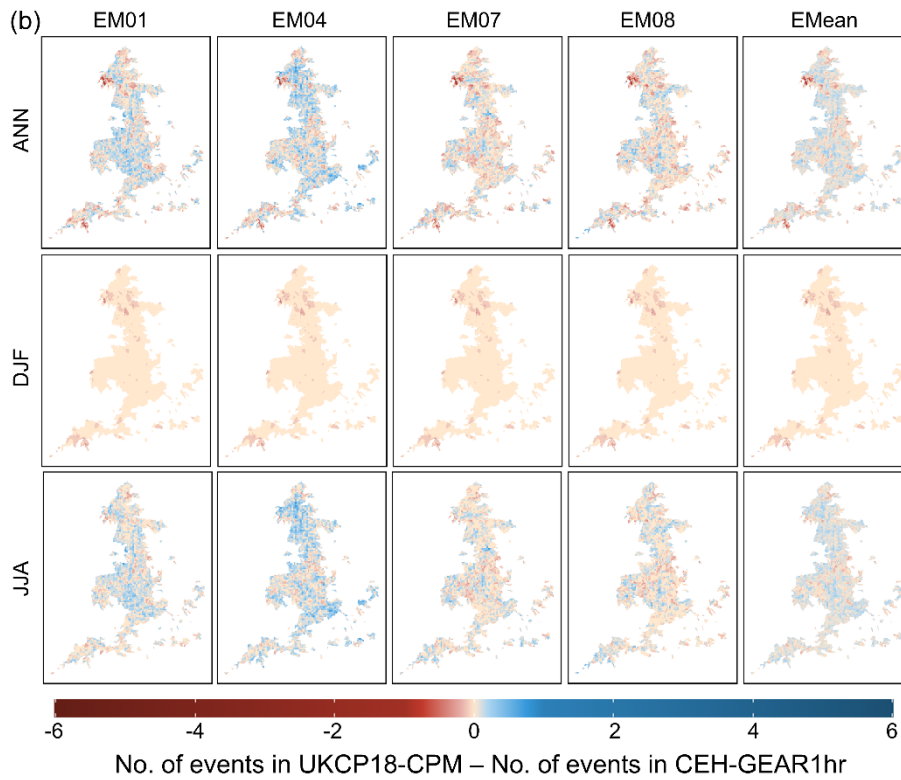
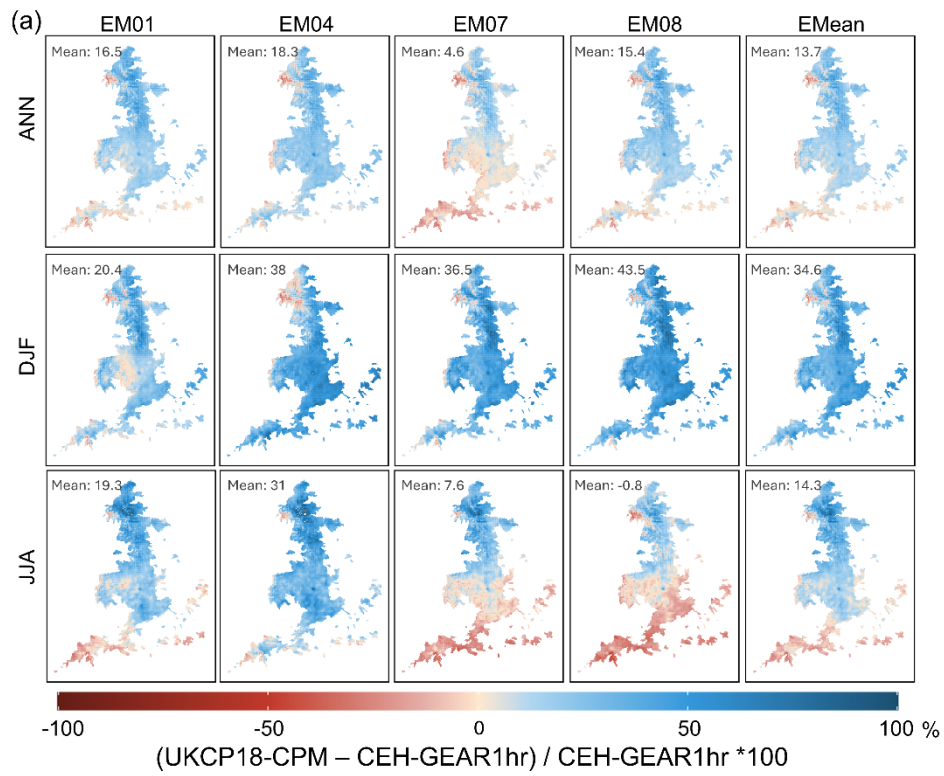
#### 3.1 Bias of raw simulations

Figure 2a shows the spatial distribution of relative biases (%) in mean hourly precipitation in the raw UKCP18-CPM simulations compared with CEH-GEAR1hr for the reference period. Figure 2b shows the change in the number of hourly rainfall events exceeding  $20 \text{ mm h}^{-1}$  in UKCP18-CPM relative to CEH-GEAR1hr over the reference period. The  $20 \text{ mm h}^{-1}$  threshold is commonly used as an indicator of potential flash flood producing rainfall in the UK (e.g., Kendon et al., 2023). The figure includes data from four ensemble members (EM01, EM04, EM07, EM08) and the ensemble mean (EMean). The figure is structured into three rows representing different temporal scales: annual bias (ANN, top row), winter season bias (DJF: December, January, February, middle row), and summer season bias (JJA: June, July, August, bottom row). A positive bias (blue) indicates an overestimation of precipitation, leading to wetter conditions, while a negative bias (red) indicates an underestimation, resulting in drier conditions.

From a spatial perspective, the annual bias (ANN) shows a consistent pattern across the four ensemble members, with wetter biases in the north and drier biases in the south. This north–south contrast is clearer in seasonal results than in the annual mean. The numerical biases for the annual average range from 4.6% (EM07) to 18.3% (EM04), indicating an overall overestimation of precipitation throughout the year.

In the winter season (DJF), biases are overall higher than those observed annually, with values ranging from 20.4% (EM01) to 43.5% (EM08). This suggests that the UKCP18-CPM tends to overestimate precipitation during winter across all four ensemble members. Spatially, the north-south contrast persists, with the northern regions generally showing wetter biases compared to the southern regions, although this gradient is not as pronounced as in the summer months. The general increase in wet bias across England during DJF implies a systematic overestimation of winter precipitation by the model.

The summer season (JJA), however, reveals the most distinct spatial gradient among four ensemble members, with a clear north-wet and south-dry pattern visible across all of them. The biases during JJA range from -0.8% (EM08) to 31% (EM04). The biases in the frequency of hourly events exceeding  $20 \text{ mm h}^{-1}$  (Fig. 2b) are generally low, which indicates that the UKCP18-CPM captures the occurrence of extreme rainfall events reasonably well, particularly in winter.



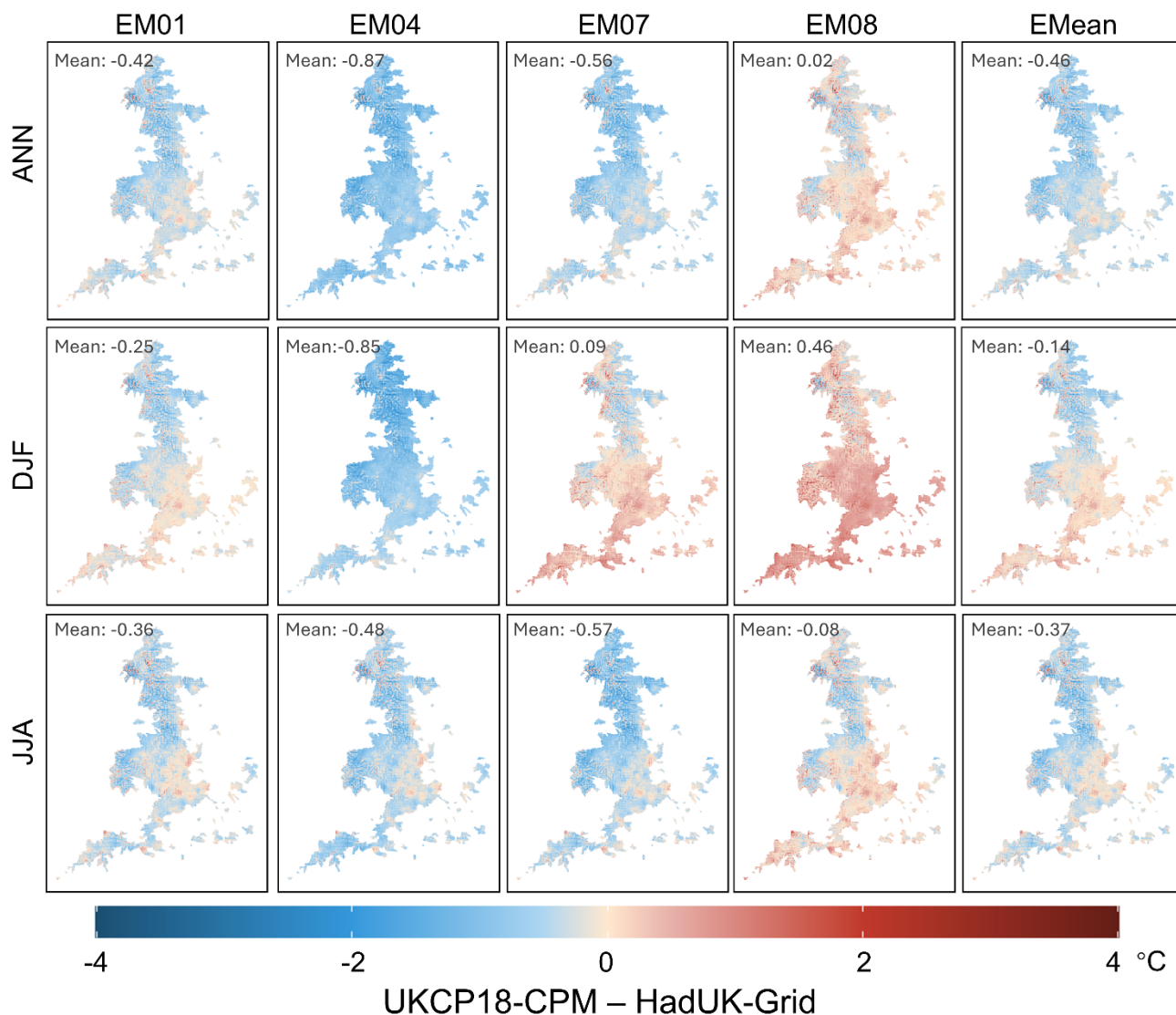
285 **Figure 2: Spatial distribution of (a) relative biases (%) in mean hourly precipitation between UKCP18-CPM and CEH-GEAR1hr and (b) differences in the number of events exceeding 20 mm h<sup>-1</sup> between UKCP18-CPM and CEH-GEAR1hr during the reference period across England. Rows represent annual (ANN), winter (DJF: December, January, February), and summer (JJA: June, July, August) results, while columns show individual ensemble members (EM01, EM04, EM07, EM08) and the ensemble mean (EMean). Blue indicates positive (wetter) biases and red indicates negative (drier) biases.**

Figure 3 shows the spatial distribution of biases in daily mean temperature from the UKCP18-CPM datasets for the reference period (December 1990 to November 2000). Each panel represents a different ensemble member (EM01, EM04, EM07, and 290 EM08) and the ensemble mean (EMean). A positive bias (red) indicates an overestimation of temperature by the UKCP18-CPM, while a negative bias (blue) indicates an underestimation, compared to HadUK-Grid observations.

For the annual mean temperature (ANN), the ensemble members show a generally cool bias across England relative to HadUK-Grid, with mean biases ranging from -0.87 °C (EM04) to +0.02 °C (EM08). Three out of the four members have negative mean biases. The spatial distribution of the annual temperature bias shows that the UKCP18-CPM generally 295 predicts lower temperatures in the northern regions of England, while the southern regions show a tendency towards a warmer bias.

During winter (DJF), the temperature biases vary more clearly across ensemble members. EM04 exhibits a cold bias of -0.85 °C, whereas EM08 shows a warm bias of 0.46 °C, indicating marked inter-member differences in winter temperature bias. The spatial distribution of winter biases is consistent with the annual trend, where the northern regions are generally 300 colder in the model compared to the observed values, while some areas in the south exhibit a warmer bias. However, the contrast between ensemble members is evident, with EM07 showing only a slight positive bias (0.09 °C), indicating that the model's performance in simulating winter temperatures varies considerably between ensemble members.

For the summer season (JJA), all four ensemble members display a cooler bias. The biases range from -0.57 °C (EM07) to -0.08 °C (EM08), suggesting that the UKCP18-CPM tends to underestimate summer temperatures. The spatial pattern during 305 JJA shows a clear north–south gradient, with stronger cooling biases in northern England and smaller biases in the south, a pattern that is consistent across all ensemble members.

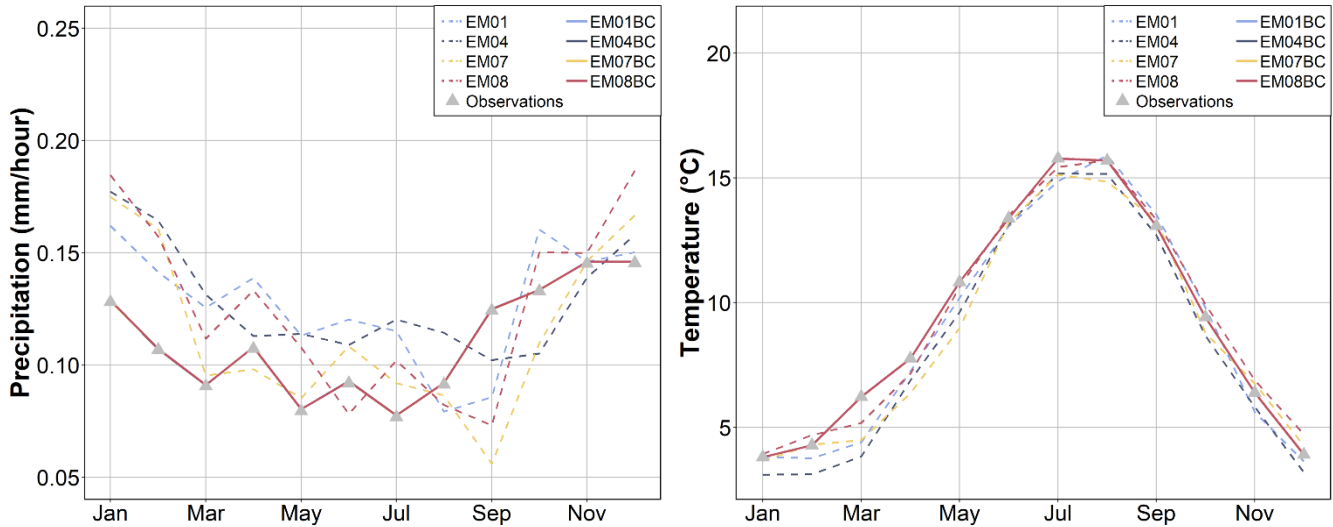


310 **Figure 3: Temperature biases (°C) in UKCP18-CPM for the reference period (December 1990 to November 2000) over England. The panels show biases for each ensemble member (EM01, EM04, EM07, and EM08) and the ensemble mean (EMean). Rows represent different time scales: annual (ANN), winter (DJF: December, January, February), and summer (JJA: June, July, August). Red indicates positive (warmer) biases and blue indicates negative (cooler) biases.**

### 3.2 Evaluation of bias correction

315 Figure 4 compares observed data with UKCP18-CPM simulations before and after bias correction for monthly precipitation (left, mm h<sup>-1</sup>) and temperature (right, °C) during the reference period (December 1990 to November 2000). Dashed lines represent raw (uncorrected) ensemble members (EM01, EM04, EM07, EM08), while solid lines indicate bias-corrected data (EM01BC, EM04BC, EM07BC, EM08BC). Observed values are marked with triangular symbols.

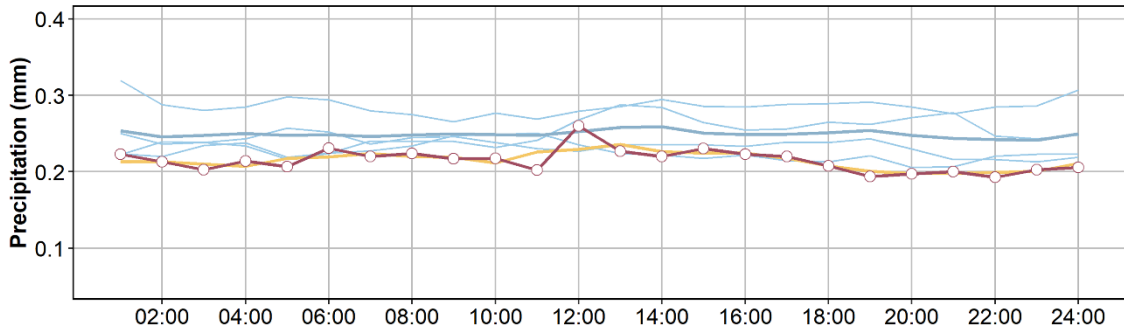
In the precipitation panel (left), the raw ensemble members deviate from observed values, particularly in winter and late summer. After bias correction, the solid lines align closely with observations, indicating effective reduction of errors. In the temperature panel (right), raw ensemble members also show noticeable deviations, especially during spring and winter. Bias correction improves the match, with the bias-corrected outputs closely following the observed temperatures throughout the year. Overall, Fig. 4 shows that bias correction effectively aligns both precipitation and temperature simulations with observed data, reducing systematic discrepancies and improving the reliability of the UKCP18-CPM outputs.



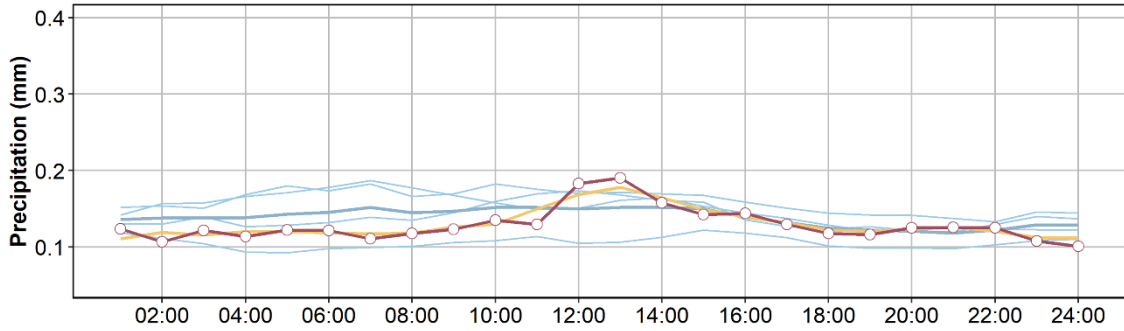
325 **Figure 4: Comparison of monthly precipitation (left,  $\text{mm/h}^{-1}$ ) and temperature (right,  $^{\circ}\text{C}$ ) between observed data and UKCP18-CPM simulations, before and after bias correction, for the reference period (December 1990 to November 2000). The blue, dark blue and yellow solid lines in both the precipitation and temperature panels lie underneath the red line.**

Figure 5 demonstrates the effectiveness of the diurnal bias correction method (DBC) in adjusting the diurnal cycle of precipitation for the reference period (December 1990 to November 2000). The blue lines represent the UKCP18-CPM four ensemble members before bias correction, where the diurnal cycle exhibits noticeable discrepancies compared to CEH-GEAR1hr (depicted by the red line with circles). Specifically, the uncorrected ensemble tends to overestimate precipitation during most hours in winter, with the ensemble mean (darker blue line) consistently showing higher precipitation compared to the observations. In contrast, during summer and autumn, the uncorrected ensemble generally underestimates precipitation across most hours. After DBC, the yellow lines (UKCP18-CPM ensemble BC) illustrate significant improvements, with the corrected ensemble mean (thicker yellow line) closely aligning with the observed diurnal cycle's temporal distribution and overall magnitude. Despite these improvements, some residual discrepancies remain, particularly in the smoother appearance of the bias-corrected results compared to CEH-GEAR1hr. These discrepancies are mainly related to the 3 h moving window used in the DBC process, which pools data from the target hour and its neighbouring hours to stabilise the hour-of-day correction.

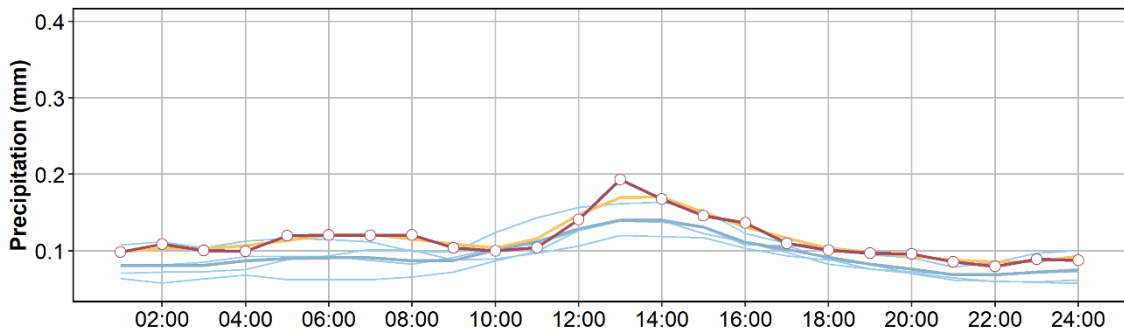
Winter (December, January, February)



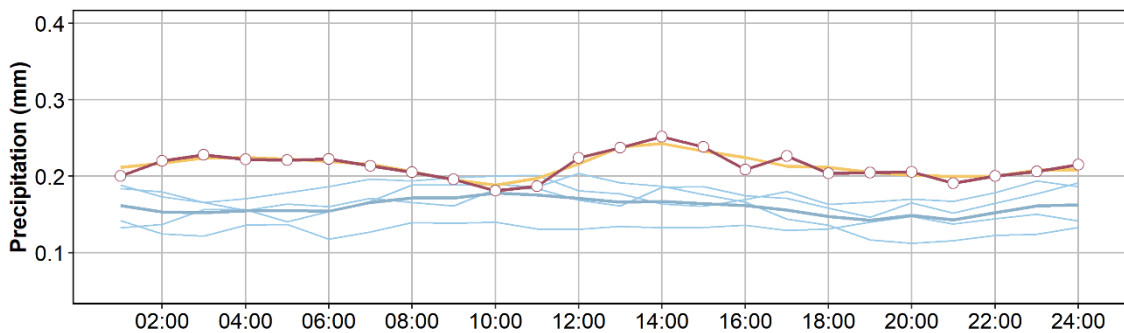
Spring (March, April, May)



Summer (June, July, August)



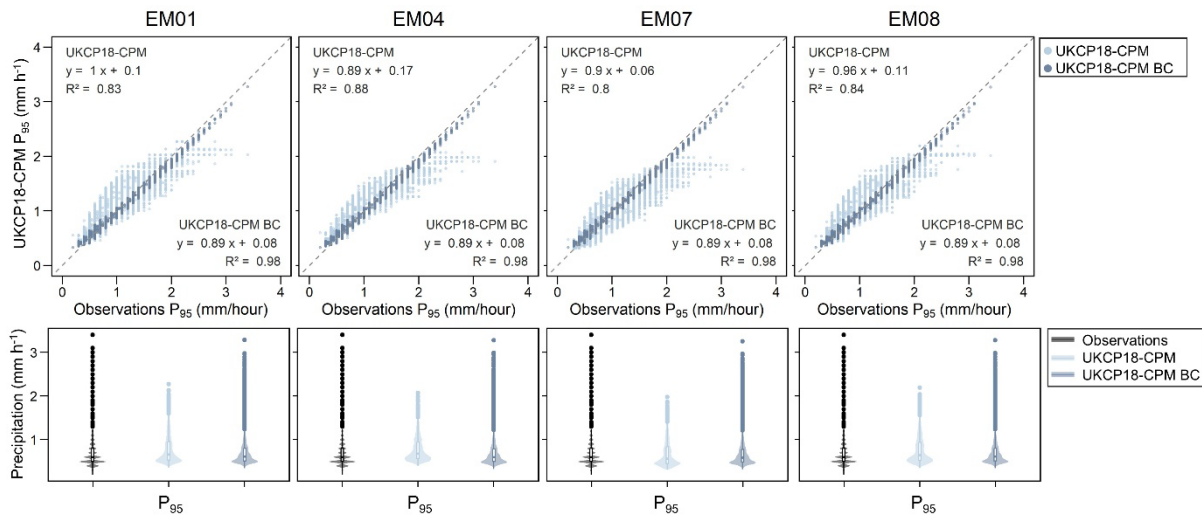
Autumn (September, October, November)



UKCP18-CPM ensemble      UKCP18-CPM ensemble BC      CEH-GEAR1hr  
UKCP18-CPM ensemble mean      UKCP18-CPM ensemble mean BC

340 **Figure 5: Diurnal cycle of mean hourly precipitation before bias correction (blue lines: UKCP18-CPM ensemble) and after bias correction (yellow lines: UKCP18-CPM ensemble BC) for the reference period. The CEH-GEAR1hr (observations) are shown as a red solid line with circles. The ensemble mean before bias correction is shown as a darker blue line (UKCP18-CPM ensemble mean), and the bias-corrected ensemble mean is shown as a darker yellow line (UKCP18-CPM ensemble mean BC). The thin yellow lines (individual members) are overlain by the thick yellow line (ensemble mean), as the diurnal cycles are similar across**  
 345 **the four members.**

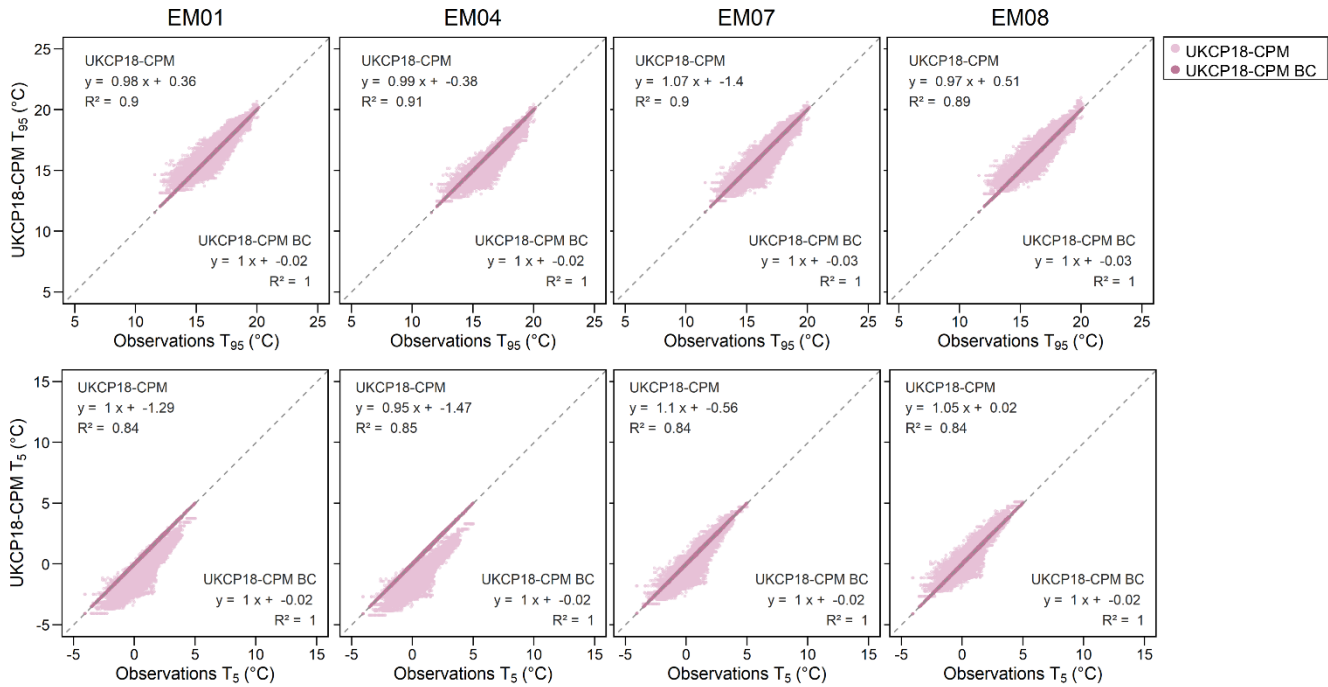
To evaluate the bias-corrected precipitation extremes in the UKCP18-CPM dataset, the 95th percentile ( $P_{95}$ ) of hourly precipitation for the reference period was calculated and compared to that of the CEH-GEAR1hr dataset (observations), as shown in Fig. 6. Here, the percentile refers to the percentile value itself (i.e., the threshold value), rather than to all values above or below that threshold. The top row displays scatter plots of the  $P_{95}$  values from UKCP18-CPM against CEH-GEAR1hr for each ensemble member, both before (light blue) and after (dark blue) bias correction. The closer the points are to the  $x=y$  line, the better the correspondence between the UKCP18-CPM and observations, indicating higher model accuracy. Initially, the raw UKCP18-CPM data shows a fair correlation with the observations, with gradients between 0.89 to 1 and  $R^2$  values ranging from 0.80 to 0.88, indicating some discrepancies in capturing extreme values. After bias correction, the  $R^2$  values improve to 0.98, demonstrating a much closer fit to observations. Before bias correction, the higher  $P_{95}$  values ( $>2$  mm/h) are largely underestimated by the CPM, which is shown as horizontal scatter of dots. Bias correction can correct these values closer to the observed values although still slightly underestimated. The bottom row presents violin plots of the  $P_{95}$  distributions for observations (black), raw UKCP18-CPM (light blue), and bias-corrected UKCP18-CPM (dark blue). These plots indicate that the bias correction not only adjusts the mean values but also better aligns the overall distribution of extreme precipitation with the observed data, reducing discrepancies in spread and central tendency.



360

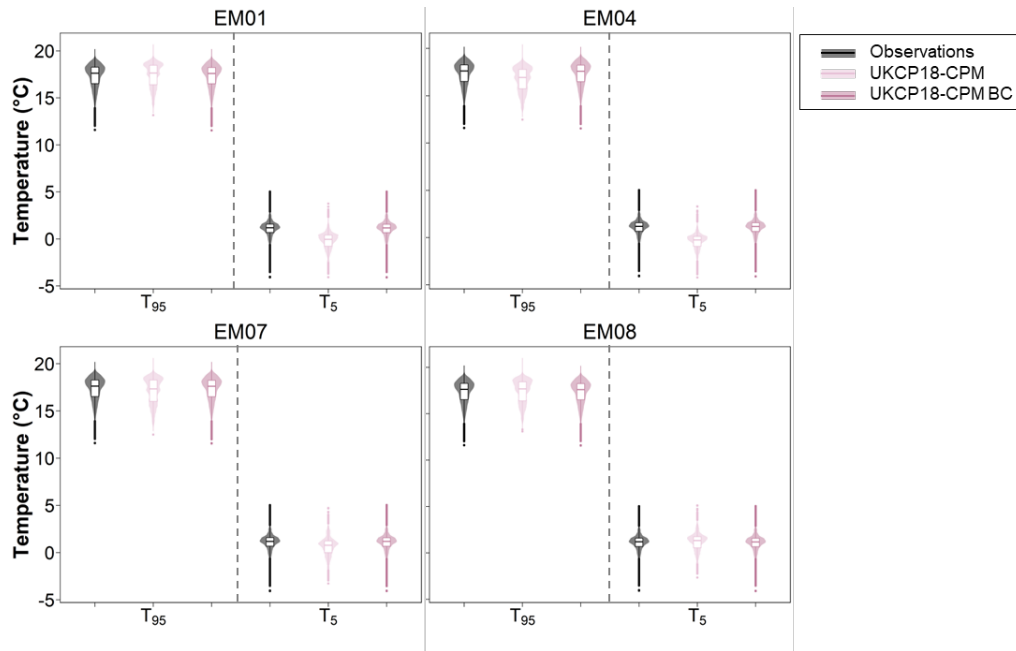
**Figure 6: Comparison of 95th percentile ( $P_{95}$ ) hourly precipitation values for the reference period. The top row shows scatter plots of UKCP18-CPM  $P_{95}$  values for each ensemble member, plotted against CEH-GEAR1hr observations for each 1 km grid, with raw (light blue) and bias-corrected (dark blue) data. The bottom row presents violin plots of  $P_{95}$  values for observations (black), raw UKCP18-CPM (light blue), and bias-corrected (dark blue) data.**

365 Temperature extremes were evaluated by comparing the 95th ( $T_{95}$ ) and 5th ( $T_5$ ) percentiles of daily mean temperature in UKCP18-CPM with HadUK-Grid for the reference period. Figure 7 shows grid-cell scatter plots ( $T_{95}$  in the top row and  $T_5$  in the bottom row) for each ensemble member, while Fig. 8 summarises the distributions using violin plots. For both  $T_{95}$  and  $T_5$ , the raw model outputs (light pink) show a fair level of correlation with the observations, with gradient values ranging from 0.97 to 1.1 and  $R^2$  values between 0.84 and 0.91. This indicates reasonable agreement, but also some discrepancies, particularly in capturing the temperature extremes. After bias correction, the fitted slope and  $R^2$  values for all four ensemble members are close to 1 in the reference period. Figure 8 complements this analysis by displaying violin plots of the distributions of  $T_{95}$  and  $T_5$  for the observations (black), raw UKCP18-CPM (light pink), and bias-adjusted UKCP18-CPM (dark pink). The plots for  $T_{95}$  (left side) and  $T_5$  (right side) clearly show that bias correction not only adjusts the central tendencies of the temperature extremes but also adjusts their distribution.



375

**Figure 7: The 95th ( $T_{95}$ , top row) and 5th ( $T_5$ , bottom row) percentile values of daily mean temperature for each ensemble member, plotted against HadUK-Grid (observations). Raw UKCP18-CPM (light pink) and bias-corrected UKCP18-CPM (dark pink) values are compared for the reference period.**



380 **Figure 8: Violin plots of  $T_{95}$  and  $T_5$  values for observations (HadUK-Grid, black), raw UKCP18-CPM (light pink), and bias-corrected UKCP18-CPM (dark pink) for each ensemble member during the reference period.**

### 3.3 Projected changes of bias-corrected UKCP18-CPM

Figures 9 and 12a illustrate the projected percentage changes in hourly precipitation from bias-corrected UKCP18-CPM simulations, comparing future periods to baseline data (2030s in Fig. 9a and 2070s in Fig. 9b). The changes are presented for both annual maximum 1 h precipitation (Rx1h) and annual total precipitation (Ptot).  
385

For the 2030s (Figs. 9a and 12a), the projections show an increase in Rx1h precipitation across all four ensemble members, with percentage changes ranging from approximately 19.9% (EM04) to 23.9% (EM08). Ptot also increases, but the changes are less pronounced, with values of 3% (EM08) and 9.4% (EM01). This suggests increases can be disproportionately higher in the extreme precipitation events than in the annual totals. By the 2070s (Figs. 9b and 12a), the projected increase in Rx1h  
390 becomes even more pronounced, with percentage changes ranging from approximately 25.1% (EM07) to 39.1% (EM04), indicating a substantial intensification of maximum hourly precipitation. In contrast, the changes in Ptot remain variable, with EM01 showing a decrease of 0.4%, confirming it as the driest member. EM04 and EM07 indicate wetter conditions, with increases of 8% and 6.1%, respectively, while EM08 shows a more moderate increase of 1.9%, representing a balanced response among the ensemble members.

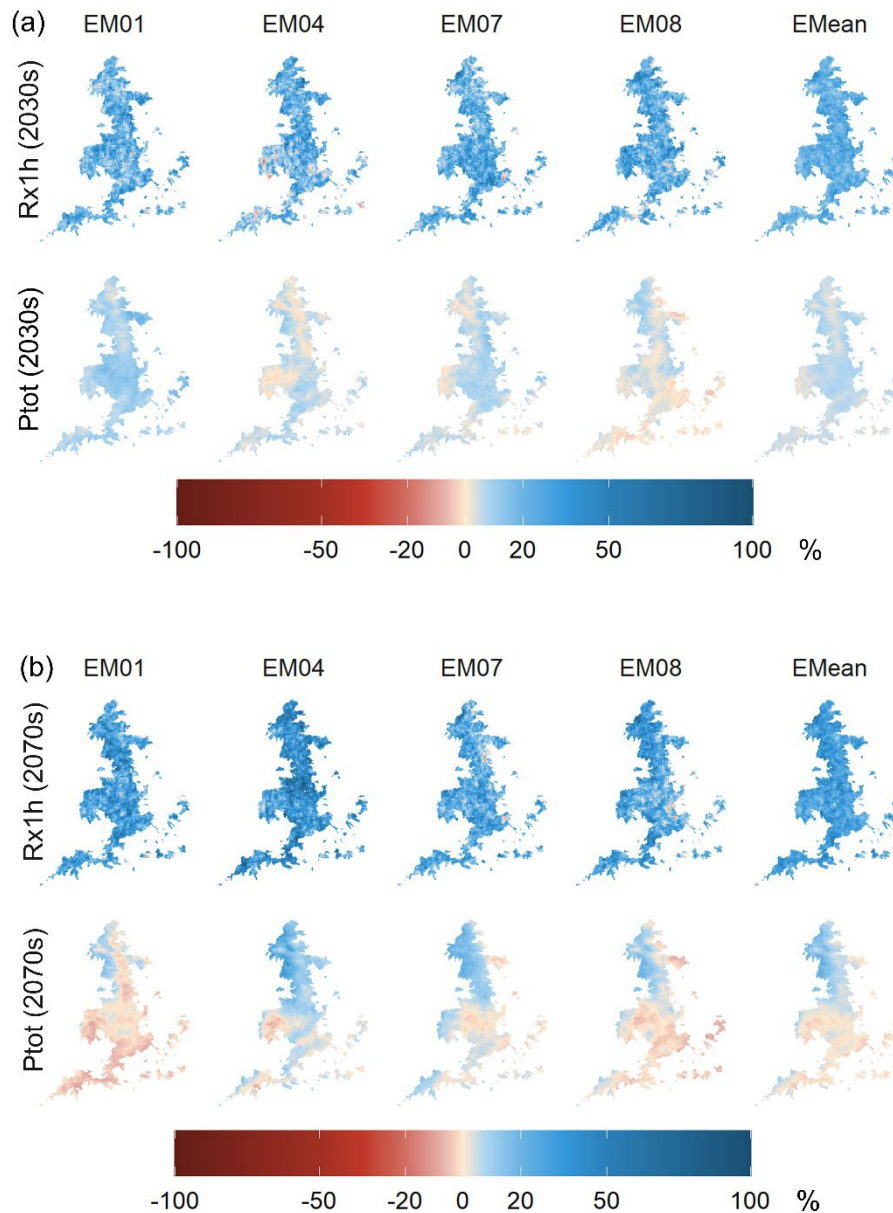


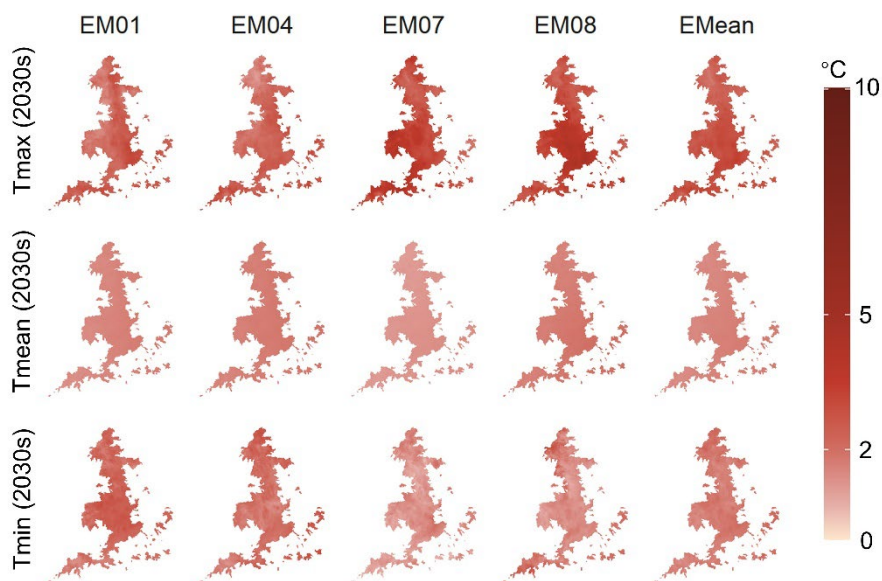
**Figure 9: Projected percentage changes in annual maximum 1 h precipitation (Rx1h) and annual total precipitation (Ptot) from bias-corrected UKCP18-CPM simulations for the (a) 2030s and (b) 2070s, compared with the baseline period.**

Figures 10 and 12b illustrate the projected percentage changes in daily mean temperature from bias-corrected UKCP18-CPM simulations, comparing baseline period data to the future periods of the 2030s (Fig. 10) and the 2070s (Fig. 11). The projections are shown for annual maximum (Tmax), annual mean (Tmean), and annual minimum (Tmin) temperatures. For the 2030s (Figs. 10 and 12b), all four ensemble members project increases in Tmax, ranging from approximately 2.2 °C (EM01) to 3.2 °C (EM08). The Tmean also shows consistent increases across ensemble members, with values ranging from

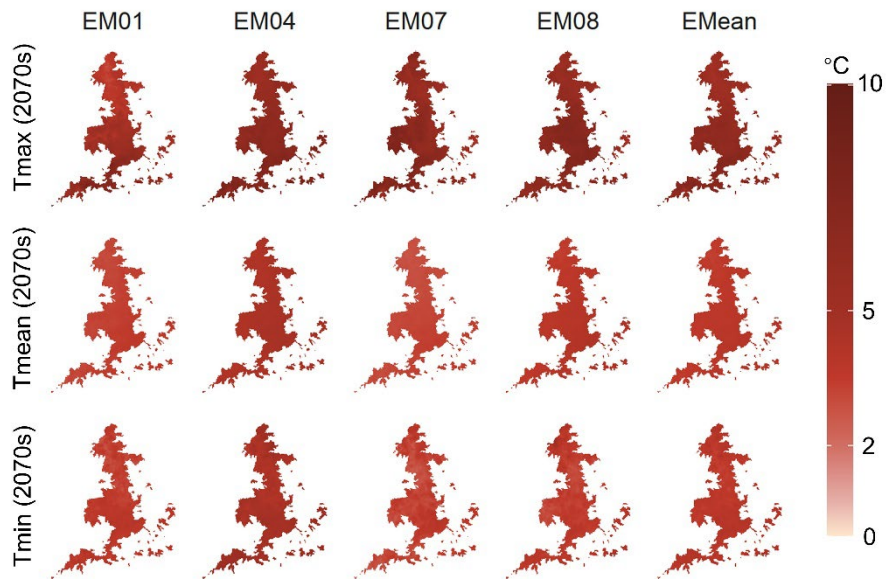
395

400

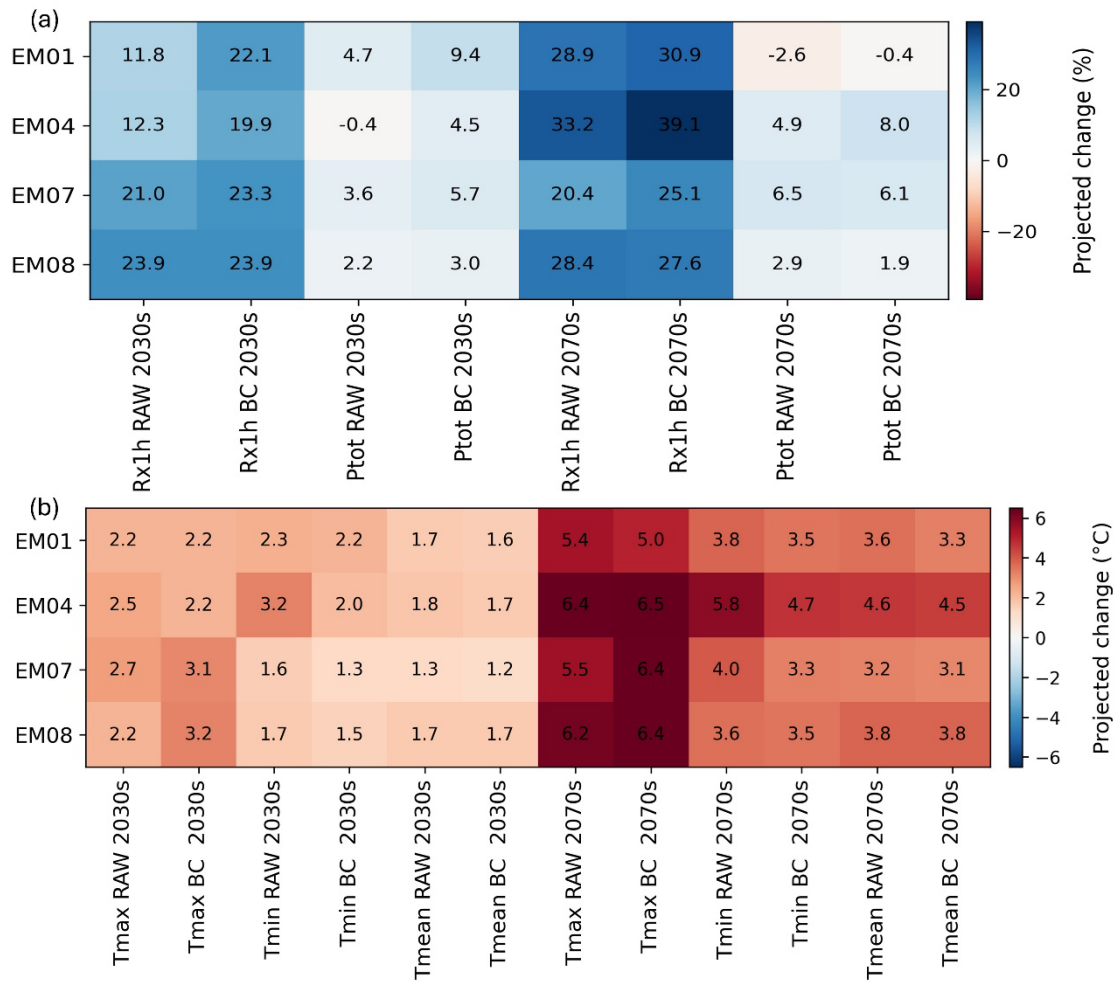
1.2 °C (EM07) to 1.7 °C (EM08). The Tmin changes are also positive, ranging from 1.3 °C (EM07) to 2.2 °C (EM01), indicating an overall warming trend in the near future. By the 2070s (Figs. 11 and 12b), the increase in Tmax becomes more pronounced, with changes ranging from approximately 5 °C (EM01) to 6.5 °C (EM04), suggesting an intensification of maximum temperatures. Similarly, the Tmean increases range from 3.1 °C (EM07) to 4.5 °C (EM04), and the Tmin changes range from 3.3 °C (EM07) to 4.7 °C (EM04). These results indicate substantial increases across all temperature metrics, i.e., maximum, mean, and minimum, by the 2070s. EM04 shows the highest level of warming in terms of Tmean temperature, with an increase of 4.5 °C, followed by EM08 at 3.8 °C. In contrast, EM01 and EM07 show more moderate increases in Tmean, with projected changes of 3.3 °C and 3.1 °C by the 2070s, respectively.



415 **Figure 10: Projected changes (°C) in the annual maximum (Tmax), annual mean (Tmean), and annual minimum (Tmin) of daily mean temperature from bias-corrected UKCP18-CPM simulations. Results are shown for the 2030s relative to the baseline period, for each processed grid cell within the analysis mask. Columns show individual ensemble members (EM01, EM04, EM07, and EM08) and the ensemble mean (EMean).**



420 **Figure 11: Projected changes (°C) in the annual maximum (Tmax), annual mean (Tmean), and annual minimum (Tmin) of daily mean temperature from bias-corrected UKCP18-CPM simulations. Results are shown for the 2070s relative to the baseline period, for each processed grid cell within the analysis mask. Columns show individual ensemble members (EM01, EM04, EM07, and EM08) and the ensemble mean (EMean).**



425 **Figure 12: Projected changes in (a) annual maximum 1 h precipitation (Rx1h) and annual total precipitation (Ptot), and (b) annual maximum (Tmax), annual mean (Tmean), and annual minimum (Tmin) of daily mean temperature for UKCP18-CPM simulations before (RAW) and after bias correction (BC). Each value is the spatial average over the processed grid cells, shown for the 2030s and 2070s relative to the baseline period.**

#### 4 Discussion

430 This study provides a practical and reproducible bias correction approach for UKCP18-CPM hourly precipitation and daily mean temperature over England and evaluates how the adjusted outputs compare with observational reference datasets across mean behaviour, diurnal characteristics, and extremes. A set of bias-corrected 1 km UKCP18-CPM temperature and precipitation projections for England is provided, using empirical quantile mapping (QM) for daily mean temperature and diurnal bias correction (DBC) for hourly precipitation. The methodological contribution is not the development of a new bias-correction method, but the transparent implementation and assessment of established quantile-mapping methods for a

large CPM dataset at hourly resolution. This is relevant for impact applications where modelled rainfall timing and intensity  
435 can strongly influence simulated responses, especially for fast-response impact applications (e.g., short-duration rainfall-  
driven flooding). These results add evidence on the value of diurnal-cycle bias correction for sub-daily precipitation in  
convection-permitting simulations, a setting where such evaluations remain relatively limited.

We applied empirical QM to daily mean temperature to address seasonal biases and distributional differences using a  
reproducible procedure. It is widely used because it can correct not only mean biases but also biases in variability and  
440 quantiles (Fang et al., 2015; Themeßl et al., 2011; Wilcke et al., 2013). For hourly precipitation, we used DBC by hour of  
day, because applying a single mapping across all hours can overlook systematic diurnal-cycle biases in sub-daily  
precipitation. Figure 5 supports this choice, showing that the bias-corrected ensemble more closely reproduces the observed  
hour-of-day pattern. This hour-of-day treatment is intended to reduce discrepancies that matter for sub-daily impact  
applications, consistent with the broader argument that correcting the diurnal cycle can improve sub-daily bias-correction  
445 strategies (Faghih et al., 2022). Therefore, we recommend using DBC for sub-daily variables. However, in this study we  
applied a 3 h moving window in the DBC. By incorporating hourly data from the previous and following hours, this may  
have contributed to some of the remaining discrepancies. It may be worth exploring whether omitting the moving window  
gives better results when the training period sample size is sufficiently large.

Before bias correction, the UKCP18-CPM simulations show considerable biases in both precipitation and temperature across  
450 various temporal and spatial scales. In general, UKCP18-CPM simulations show wet precipitation biases (especially in  
winter) and cool biases in temperature. These broad patterns are consistent with previous evaluations of UKCP18-RCM  
simulations (Reyniers et al., 2025) and the UKCP18-CPM science report (Kendon et al., 2019b). These residual biases are  
consistent with the broader CPM literature, which shows that although kilometre-scale models can improve the  
representation of precipitation compared with convection-parameterised RCMs, systematic biases and model uncertainty  
455 may remain, particularly for sub-daily precipitation and across different regional settings (Ban et al., 2021; Correa-Sánchez  
et al., 2025; Soares et al., 2024). After bias correction, both precipitation and temperature show substantially improved  
agreement with observations at monthly and diurnal timescales (Figs. 4 and 5). This suggests that bias correction provides a  
more reliable basis for downstream impact assessments than raw UKCP18-CPM output.

Future changes were also analysed for both precipitation and temperature in Figs. 9–12. In general, the bias-corrected  
460 projections indicate a clear intensification of annual maximum 1 h precipitation (Rx1h) by both the 2030s and 2070s, while  
changes in annual total precipitation (Ptot) remain smaller and spatially variable (Figs. 9 and 12). This pattern (i.e., stronger  
changes in short-duration extremes than in totals) is broadly consistent with CPM-based studies that report amplified  
changes for sub-daily extremes and a strong dependence on dynamical factors and regional setting (Dallan et al., 2024;  
Pichelli et al., 2021). The projected temperature changes are consistent with findings from the UKCP18-CPM science report  
465 (Kendon et al., 2019b), which indicated that mean temperature is expected to increase across all regions and seasons. Our  
findings also align well with existing literature, such as Robinson et al. (2023), who reported similar projected changes for

UKCP18-RCM. This suggests that the bias-corrected projections remain broadly consistent with previously reported climate change signals.

470 Due to limitations in computational resources and time, we focused our analysis on four ensemble members: EM01, EM04, EM07, and EM08. These were selected to represent a diverse range of climate outcomes, from the driest to the wettest scenarios, allowing the bias-corrected dataset to effectively capture the range of possible climate responses in England. This sub-ensemble was chosen to balance computational efficiency with representativeness while ensuring that the selection captures a wide range of precipitation responses. The reduced number of ensemble members may influence the ensemble mean and spread compared to using all 12 members. Future studies could address this by expanding the bias correction to include more ensemble members and broader spatial coverage. Additionally, the integration of multivariate bias correction methods (Cannon, 2018; Faghih et al., 2022) could offer the advantage of preserving inter-variable dependencies, ensuring that precipitation and temperature are corrected consistently without disrupting their natural relationship.

480 This high-resolution bias-corrected dataset offers enhanced reliability, making it suitable for a wide range of climate change impact simulations and studies. The dataset's fine spatial and temporal resolution enables its application in various fields, such as flood forecasting, agricultural planning, and natural resource management, providing valuable insights for decision-making and long-term adaptation strategies. Future research could extend this analysis to other regions and incorporate additional climate models, providing a broader understanding of the impacts of climate change and helping to assess the applicability of these methods in different contexts. This would not only improve the robustness of climate projections but also enhance the relevance and utility of bias-corrected datasets in informing climate adaptation strategies.

## 485 **5 Conclusions**

In this study, we applied bias correction to the UKCP18 Convection-Permitting Model (CPM) data to produce 1 km high-resolution precipitation and temperature projections for England, UK. Using quantile mapping (QM) as our bias correction method, we corrected biases in hourly precipitation and daily temperature data for four ensemble members (EM01, EM04, EM07, and EM08) selected to represent the spread of the full ensemble. Our results demonstrate that bias correction improved the alignment of UKCP18-CPM simulations with observational datasets, effectively reducing discrepancies (biases) and enhancing the model's performance across various metrics. The bias-corrected dataset provides a more reliable foundation for assessing future climatic changes and regional impacts across England. Although the bias-correction approaches applied here are established, this study provides new evidence of their performance for sub-daily precipitation in convection-permitting UK climate projections, including improvements in diurnal-cycle behaviour and sub-daily extremes relevant to impact modelling. The key findings are as follows:

1. Raw UKCP18-CPM simulations showed consistent wet biases for precipitation and cooler biases for temperature. For precipitation, the annual average biases ranged from 4.6% (EM07) to 18.3% (EM04), with the largest biases occurring in winter (DJF) ranging from 20.4% (EM01) to 43.5% (EM08). Temperature biases show a clear seasonal

dependence, with winter (DJF) exhibiting larger spatial contrasts and summer (JJA) showing a more consistent cool bias across all members. On an annual mean basis, the temperature bias ranged from  $-0.87$  °C (EM04) to  $+0.02$  °C (EM08), with three of the four members showing a cool bias.

2. After bias correction, both precipitation and temperature simulations aligned well with observational data. Monthly precipitation and temperature biases were substantially reduced, with bias corrected outputs closely following observed monthly patterns. The diurnal cycle of bias corrected precipitation captured the variability and magnitude of observed precipitation across most hours of the day. The 95th percentile ( $P_{95}$ ) of hourly precipitation and temperature extremes ( $T_{95}$ ) showed markedly improved agreement with observations after bias correction for both mean behaviour and high-percentile extremes ( $P_{95}$  and  $T_{95}$ ).
3. Future projections for the 2030s and 2070s show significant increases in both precipitation and temperature. By the 2030s, annual maximum 1 h precipitation ( $Rx1h$ ) is projected to increase by 19.9% (EM04) to 23.9% (EM08), while annual total precipitation ( $P_{tot}$ ) shows more moderate increases, ranging from 3% (EM08) to 9.4% (EM01). In terms of temperature, annual mean temperature ( $T_{mean}$ ) increases range from 1.2 °C (EM07) to 1.7 °C (EM08) by the 2030s. By the 2070s, these trends become more pronounced, with  $Rx1h$  increasing by 25.1% (EM07) to 39.1% (EM04), and  $T_{mean}$  projected to rise by 3.1 °C (EM07) to 4.5 °C (EM04). These projections indicate a potential for more intense extreme weather events, particularly for precipitation and temperature extremes, as the century progresses.

## Appendix A

**Table A1. NRFA ID of the selected 249 catchments**

Catchment ID												
22006	27025	28003	28072	32008	37019	40004	43009	47014	52007	54011	55002	71006
22009	27026	28008	28074	33018	37020	40009	44001	47018	52009	54012	55013	71008
23001	27029	28009	28080	33019	37033	40011	44006	48003	52010	54016	55014	72002
23004	27030	28012	28081	33028	38007	40021	45001	48004	52011	54018	55018	72004
23008	27034	28018	28082	33031	38014	41001	45003	48005	52015	54019	68001	72007
23011	27035	28023	28085	33039	38018	41005	45004	48011	52016	54020	68003	72015
23016	27041	28024	28091	33058	39002	41006	45005	49001	53007	54027	68005	73005
24001	27042	28026	28093	34002	39005	41009	45009	49002	53008	54029	68020	73009
24004	27043	28031	28117	34005	39021	41011	45012	49004	53009	54034	69007	73010
24005	27047	28039	29003	34006	39034	41012	46003	50001	53017	54036	69012	73011
25001	27049	28040	30001	34007	39042	41013	46005	50002	53018	54038	69015	74001

25003	27051	28043	30004	34010	39052	41025	46008	50006	53023	54048	69017	74006
25020	27064	28046	30005	35008	39069	41027	46014	50007	53028	54049	69023	74007
26008	27071	28048	30011	36006	39087	41028	47001	50008	54001	54052	69027	75003
27001	27077	28052	30012	36011	39095	41029	47004	50011	54002	54057	69030	75004
27002	27080	28055	31010	36012	39099	42003	47005	51001	54004	54060	69032	75017
27003	27084	28056	31023	37008	39105	42017	47008	52004	54005	54063	69043	76007
27007	27089	28066	32003	37009	39143	43005	47009	52005	54007	54095	71001	76011
27021	27090	28067	32006	37018	39144	43007	47011	52006	54008	54096	71004	76014
101002	101005											

---

*Data availability.* The dataset is available at Zenodo (<https://zenodo.org/records/16213003>).

520

*Author contributions.* QZ performed most of the computational tasks and data curation. She performed most of the formal analysis and investigations and drafted the manuscript. NF assisted with writing bias correction program scripts. YH and TO provided guidance for the analysis and interpretation of the results. All authors reviewed the final manuscript and contributed to the writing.

525

*Competing interests.* The authors declare no competing financial or non-financial interests. One of the co-authors Yi He serves as an editor for Hydrology and Earth System Sciences (HESS).

*Acknowledgements.* The authors are grateful for the support provided by the high-performance Linux compute cluster at the University of East Anglia, which was used to conduct the bias correction in this study. We would also like to express our gratitude to Lukas Gudmundsson, the developer of the QM R package 'qmap,' for providing this valuable tool. Furthermore, we thank the Met Office for making the HadUK-Grid and UKCP18-CPM datasets available, and the UK Centre for Ecology & Hydrology for access to the CEH-GEAR1hr dataset.

*Financial support.* This work was supported by the Open CLimate IMpacts modelling framework (OpenCLIM) project funded by the UK Natural Environment Research Council award number NE/T013931/1.

## References

Ayugi, B., Tan, G., Ruoyun, N., Babausmail, H., Ojara, M., Wido, H., Mumo, L., Ngoma, N. H., Nooni, I. K., and Ongoma, V.: Quantile Mapping Bias Correction on Rossby Centre Regional Climate Models for Precipitation Analysis over Kenya, East Africa, *Water*, 12, 801, <https://doi.org/10.3390/w12030801>, 2020.

- Ban, N., Schmidli, J., and Schär, C.: Evaluation of the convection-resolving regional climate modeling approach in decade-long simulations, *Journal of Geophysical Research: Atmospheres*, 119, 7889–7907, <https://doi.org/10.1002/2014JD021478>, 2014.
- 545 Ban, N., Caillaud, C., Coppola, E., Pichelli, E., Sobolowski, S., Adinolfi, M., Ahrens, B., Alias, A., Anders, I., Bastin, S., Belušić, D., Berthou, S., Brisson, E., Cardoso, R. M., Chan, S. C., Christensen, O. B., Fernández, J., Fita, L., Frisius, T., Gašparac, G., Giorgi, F., Goergen, K., Haugen, J. E., Hodnebrog, Ø., Kartsios, S., Katragkou, E., Kendon, E. J., Keuler, K., Lavin-Gullon, A., Lenderink, G., Leutwyler, D., Lorenz, T., Maraun, D., Mercogliano, P., Milovac, J., Panitz, H.-J., Raffa, M., Remedio, A. R., Schär, C., Soares, P. M. M., Srnec, L., Steensen, B. M., Stocchi, P., Tölle, M. H., Truhetz, H., Vergara-Temprado, J., de Vries, H., Warrach-Sagi, K., Wulfmeyer, V., and Zander, M. J.: The first multi-model ensemble of regional  
550 climate simulations at kilometer-scale resolution, part I: evaluation of precipitation, *Clim Dyn*, 57, 275–302, <https://doi.org/10.1007/s00382-021-05708-w>, 2021.
- Bannister, D., Orr, A., Jain, S. K., Holman, I. P., Momblanch, A., Phillips, T., Adeloje, A. J., Snapir, B., Waive, T. W., Hosking, J. S., and Allen-Sader, C.: Bias Correction of High-Resolution Regional Climate Model Precipitation Output Gives the Best Estimates of Precipitation in Himalayan Catchments, *Journal of Geophysical Research: Atmospheres*, 124, 14220–  
555 14239, <https://doi.org/10.1029/2019JD030804>, 2019.
- Berthou, S., Kendon, E. J., Chan, S. C., Ban, N., Leutwyler, D., Schär, C., and Fosser, G.: Pan-European climate at convection-permitting scale: a model intercomparison study, *Clim Dyn*, 55, 35–59, <https://doi.org/10.1007/s00382-018-4114-6>, 2020.
- Boé, J., Terray, L., Habets, F., and Martin, E.: Statistical and dynamical downscaling of the Seine basin climate for hydro-  
560 meteorological studies, *International Journal of Climatology*, 27, 1643–1655, <https://doi.org/10.1002/joc.1602>, 2007.
- Breidl, K. and Di Baldassarre, G.: Space-time disaggregation of precipitation and temperature across different climates and spatial scales, *Journal of Hydrology: Regional Studies*, 21, 126–146, <https://doi.org/10.1016/j.ejrh.2018.12.002>, 2019.
- Cannon, A. J.: Multivariate Quantile Mapping Bias Correction: An N-dimensional Probability Density Function Transform for Climate Model Simulations of Multiple Variables, *Climate Dynamics*, 50, 31–49, <https://doi.org/10.1007/s00382-017-3580-6>, 2018.  
565
- Cannon, A. J., Sobie, S. R., and Murdock, T. Q.: Bias Correction of GCM Precipitation by Quantile Mapping: How Well Do Methods Preserve Changes in Quantiles and Extremes?, *J. Climate*, 28, 6938–6959, <https://doi.org/10/f7p6ft>, 2015.
- Chokkavarapu, N. and Mandla, V. R.: Comparative study of GCMs, RCMs, downscaling and hydrological models: a review toward future climate change impact estimation, *SN Appl. Sci.*, 1, 1698, <https://doi.org/10.1007/s42452-019-1764-x>, 2019.
- 570 Correa-Sánchez, N., Dallan, E., Marra, F., Fosser, G., and Borga, M.: Orographic control on bias and uncertainty in extreme sub-daily precipitation simulations from a convection-permitting ensemble, *Journal of Hydrology*, 659, 133324, <https://doi.org/10.1016/j.jhydrol.2025.133324>, 2025.
- Dai, A., Giorgi, F., and Trenberth, K. E.: Observed and model-simulated diurnal cycles of precipitation over the contiguous United States, *J. Geophys. Res.*, 104, 6377–6402, <https://doi.org/10.1029/98JD02720>, 1999.
- 575 Dallan, E., Marra, F., Fosser, G., Marani, M., and Borga, M.: Dynamical Factors Heavily Modulate the Future Increase of Sub-Daily Extreme Precipitation in the Alpine-Mediterranean Region, *Earth's Future*, 12, e2024EF005185, <https://doi.org/10.1029/2024EF005185>, 2024.

- Done, J., Davis, C. A., and Weisman, M.: The next generation of NWP: explicit forecasts of convection using the weather research and forecasting (WRF) model, *Atmosph. Sci. Lett.*, 5, 110–117, <https://doi.org/10.1002/asl.72>, 2004.
- 580 Faghiih, M., Brissette, F., and Sabeti, P.: Impact of correcting sub-daily climate model biases for hydrological studies, *Hydrology and Earth System Sciences*, 26, 1545–1563, <https://doi.org/10.5194/hess-26-1545-2022>, 2022.
- Fang, G. H., Yang, J., Chen, Y. N., and Zammit, C.: Comparing bias correction methods in downscaling meteorological variables for a hydrologic impact study in an arid area in China, *Hydrology and Earth System Sciences*, 19, 2547–2559, <https://doi.org/10.5194/hess-19-2547-2015>, 2015.
- 585 Gudde, R., He, Y., Pasquier, U., Forstenhäusler, N., Noble, C., and Zha, Q.: Quantifying future changes of flood hazards within the Broadland catchment in the UK, *Nat Hazards*, 120, 9893–9915, <https://doi.org/10.1007/s11069-024-06590-5>, 2024.
- Gudmundsson, L., Bremnes, J. B., Haugen, J. E., and Engen-Skaugen, T.: Technical Note: Downscaling RCM precipitation to the station scale using statistical transformations &ndash; a comparison of methods, *Hydrol. Earth Syst. Sci.*, 16, 3383–3390, <https://doi.org/10/f4drr9>, 2012.
- 590 Gutmann, E., Pruitt, T., Clark, M. P., Brekke, L., Arnold, J. R., Raff, D. A., and Rasmussen, R. M.: An intercomparison of statistical downscaling methods used for water resource assessments in the United States, *Water Resources Research*, 50, 7167–7186, <https://doi.org/10.1002/2014WR015559>, 2014.
- Hanlon, H. M., Bernie, D., Carigi, G., and Lowe, J. A.: Future changes to high impact weather in the UK, *Climatic Change*, 50, 166, <https://doi.org/10.1007/s10584-021-03100-5>, 2021.
- 595 Hannaford, J., Mackay, J. D., Ascott, M., Bell, V. A., Chitson, T., Cole, S., Counsell, C., Durant, M., Jackson, C. R., Kay, A. L., Lane, R. A., Mansour, M., Moore, R., Parry, S., Rudd, A. C., Simpson, M., Facer-Childs, K., Turner, S., Wallbank, J. R., Wells, S., and Wilcox, A.: The enhanced future Flows and Groundwater dataset: development and evaluation of nationally consistent hydrological projections based on UKCP18, *Earth System Science Data*, 15, 2391–2415, <https://doi.org/10.5194/essd-15-2391-2023>, 2023.
- 600 Hollis, D., McCarthy, M., Kendon, M., Legg, T., and Simpson, I.: HadUK-Grid—A new UK dataset of gridded climate observations, *Geoscience Data Journal*, 6, 151–159, <https://doi.org/10.1002/gdj3.78>, 2019.
- IPCC: Climate Change 2021 – The Physical Science Basis: Working Group I Contribution to the Sixth Assessment Report of the Intergovernmental Panel on Climate Change, 1st ed., Cambridge University Press, <https://doi.org/10.1017/9781009157896>, 2023a.
- 605 IPCC: Climate Change 2022 – Impacts, Adaptation and Vulnerability: Working Group II Contribution to the Sixth Assessment Report of the Intergovernmental Panel on Climate Change, Cambridge University Press, Cambridge, <https://doi.org/10.1017/9781009325844>, 2023b.
- Kay, A. and Brown, M.: Using sub-daily precipitation for grid-based hydrological modelling across Great Britain: Assessing model performance and comparing flood impacts under climate change, *Journal of Hydrology: Regional Studies*, 50, 101588, <https://doi.org/10.1016/j.ejrh.2023.101588>, 2023.
- 610 Kay, A., Bell, V. A., Davies, H. N., Lane, R. A., and Rudd, A. C.: The UKSCAPE-G2G river flow and soil moisture datasets: Grid-to-Grid model estimates for the UK for historical and potential future climates, *Earth System Science Data*, 15, 2533–2546, <https://doi.org/10.5194/essd-15-2533-2023>, 2023.

- 615 Keller, A. A., Garner, K. L., Rao, N., Knipping, E., and Thomas, J.: Downscaling approaches of climate change projections for watershed modeling: Review of theoretical and practical considerations, *PLOS Water*, 1, e0000046, <https://doi.org/10.1371/journal.pwat.0000046>, 2022.
- Kendon, E. J., Jones, R. G., Kjellström, E., and Murphy, J. M.: Using and Designing GCM–RCM Ensemble Regional Climate Projections, *J. Climate*, 23, 6485–6503, <https://doi.org/10.1175/2010JCLI3502.1>, 2010.
- 620 Kendon, E. J., Stratton, R. A., Tucker, S., Marsham, J. H., Berthou, S., Rowell, D. P., and Senior, C. A.: Enhanced future changes in wet and dry extremes over Africa at convection-permitting scale, *Nat Commun*, 10, 1794, <https://doi.org/10.1038/s41467-019-09776-9>, 2019a.
- Kendon, E. J., Fosser, G., Murphy, J., Chan, S., Clark, R., Harris, G., Lock, A., Lowe, J., Martin, G., Pirret, J., Roberts, N., Sanderson, M., and Tucker, S.: UKCP Convection-permitting model projections: Science report, 2019b.
- 625 Kendon, E. J., Short, C., Pope, J., Chan, S., Wilkinson, J., Tucker, S., Bett, P., and Harris, G.: Update to UKCP Local (2.2km) projections, Met Office Hadley Centre, Exeter, UK, 2021.
- Kendon, E. J., Fischer, E. M., and Short, C. J.: Variability conceals emerging trend in 100yr projections of UK local hourly rainfall extremes, *Nat Commun*, 14, 1133, <https://doi.org/10.1038/s41467-023-36499-9>, 2023.
- 630 Kotlarski, S., Keuler, K., Christensen, O. B., Colette, A., Déqué, M., Gobiet, A., Goergen, K., Jacob, D., Lüthi, D., van Meijgaard, E., Nikulin, G., Schär, C., Teichmann, C., Vautard, R., Warrach-Sagi, K., and Wulfmeyer, V.: Regional climate modeling on European scales: a joint standard evaluation of the EURO-CORDEX RCM ensemble, *Geoscientific Model Development*, 7, 1297–1333, <https://doi.org/10.5194/gmd-7-1297-2014>, 2014.
- Lafon, T., Dadson, S., Buys, G., and Prudhomme, C.: Bias correction of daily precipitation simulated by a regional climate model: a comparison of methods, *International Journal of Climatology*, 33, 1367–1381, <https://doi.org/10.1002/joc.3518>, 2013.
- 635 Lean, H. W., Clark, P. A., Dixon, M., Roberts, N. M., Fitch, A., Forbes, R., and Halliwell, C.: Characteristics of High-Resolution Versions of the Met Office Unified Model for Forecasting Convection over the United Kingdom, *Mon. Wea. Rev.*, 136, 3408–3424, <https://doi.org/10.1175/2008MWR2332.1>, 2008.
- Lewis, E., Quinn, N., Blenkinsop, S., Fowler, H. J., Freer, J., Tanguy, M., Hitt, O., Coxon, G., Bates, P., Woods, R., Fry, M., Chevuturi, A., Swain, O., and White, S. M.: Gridded estimates of hourly areal rainfall for Great Britain 1990-2016 [CEH-GEAR1hr] v2, 2022.
- 640 Maraun, D., Widmann, M., and Gutiérrez, J. M.: Statistical downscaling skill under present climate conditions: A synthesis of the VALUE perfect predictor experiment, *International Journal of Climatology*, 39, 3692–3703, <https://doi.org/10.1002/joc.5877>, 2019.
- 645 Maurer, V., Bischoff-Gauß, I., Kalthoff, N., Gantner, L., Roca, R., and Panitz, H.-J.: Initiation of deep convection in the Sahel in a convection-permitting climate simulation for northern Africa, *Quarterly Journal of the Royal Meteorological Society*, 143, 806–816, <https://doi.org/10.1002/qj.2966>, 2017.
- Met Office, Hollis, D., McCarthy, M., Kendon, M., and Legg, T.: HadUK-Grid Gridded Climate Observations on a 1km grid over the UK, v1.1.0.0 (1836-2021), <https://doi.org/10.5285/BBCA3267DC7D4219AF484976734C9527>, 2022.
- 650 Met Office Hadley Centre: UKCP Local Projections on a 5km grid over the UK for 1980-2080, 2019.

- Murata, A., Sasaki, H., Kawase, H., and Nosaka, M.: Evaluation of precipitation over an oceanic region of Japan in convection-permitting regional climate model simulations, *Clim Dyn*, 48, 1779–1792, <https://doi.org/10.1007/s00382-016-3172-x>, 2017.
- 655 Murphy, J. M., Harris, G. R., Sexton, D. M. H., Kendon, E. J., Bett, P. E., Clark, R. T., Eagle, K. E., Fosse, G., Fung, F., Lowe, J. A., McDonald, R. E., McInnes, R. N., McSweeney, C. F., Mitchell, J. F. B., Rostron, J. W., Thornton, H. E., Tucker, S., and Yamazaki, K.: UKCP18 Land Projections: Science Report, Met Office Hadley Centre, UK, 2018.
- Ngai, S. T., Tangang, F., and Juneng, L.: Bias correction of global and regional simulated daily precipitation and surface mean temperature over Southeast Asia using quantile mapping method, *Global and Planetary Change*, 149, 79–90, <https://doi.org/10.1016/j.gloplacha.2016.12.009>, 2017.
- 660 Piani, C., Weedon, G. P., Best, M., Gomes, S. M., Viterbo, P., Hagemann, S., and Haerter, J. O.: Statistical bias correction of global simulated daily precipitation and temperature for the application of hydrological models, *Journal of Hydrology*, 395, 199–215, <https://doi.org/10.1016/j.jhydrol.2010.10.024>, 2010.
- 665 Pichelli, E., Coppola, E., Sobolowski, S., Ban, N., Giorgi, F., Stocchi, P., Alias, A., Belušić, D., Berthou, S., Caillaud, C., Cardoso, R. M., Chan, S., Christensen, O. B., Dobler, A., de Vries, H., Goergen, K., Kendon, E. J., Keuler, K., Lenderink, G., Lorenz, T., Mishra, A. N., Panitz, H.-J., Schär, C., Soares, P. M. M., Truhetz, H., and Vergara-Temprado, J.: The first multi-model ensemble of regional climate simulations at kilometer-scale resolution part 2: historical and future simulations of precipitation, *Clim Dyn*, 56, 3581–3602, <https://doi.org/10.1007/s00382-021-05657-4>, 2021.
- 670 Reiter, P., Gutjahr, O., Schefczyk, L., Heinemann, G., and Casper, M.: Does applying quantile mapping to subsamples improve the bias correction of daily precipitation?, *International Journal of Climatology*, 38, 1623–1633, <https://doi.org/10.1002/joc.5283>, 2018.
- Reyniers, N., Osborn, T. J., Addor, N., and Darch, G.: Projected changes in droughts and extreme droughts in Great Britain strongly influenced by the choice of drought index, *Hydrology and Earth System Sciences*, 27, 1151–1171, <https://doi.org/10.5194/hess-27-1151-2023>, 2023.
- 675 Reyniers, N., Zha, Q., Addor, N., Osborn, T. J., Forstnhäusler, N., and He, Y.: Two sets of bias-corrected regional UK Climate Projections 2018 (UKCP18) of temperature, precipitation and potential evapotranspiration for Great Britain, *Earth System Science Data*, 17, 2113–2133, <https://doi.org/10.5194/essd-17-2113-2025>, 2025.
- Riahi, K., Rao, S., Krey, V., Cho, C., Chirkov, V., Fischer, G., Kindermann, G., Nakicenovic, N., and Rafaj, P.: RCP 8.5—A scenario of comparatively high greenhouse gas emissions, *Climatic Change*, 109, 33, <https://doi.org/10.1007/s10584-011-0149-y>, 2011.
- 680 Roberts, N. M. and Lean, H. W.: Scale-Selective Verification of Rainfall Accumulations from High-Resolution Forecasts of Convective Events, *Mon. Wea. Rev.*, 136, 78–97, <https://doi.org/10.1175/2007MWR2123.1>, 2008.
- 685 Robinson, E. L., Huntingford, C., Semeena, V. S., and Bullock, J. M.: CHES-SCAPE: high-resolution future projections of multiple climate scenarios for the United Kingdom derived from downscaled United Kingdom Climate Projections 2018 regional climate model output, *Earth System Science Data*, 15, 5371–5401, <https://doi.org/10.5194/essd-15-5371-2023>, 2023.
- Sangelantoni, L., Russo, A., and Gennaretti, F.: Impact of bias correction and downscaling through quantile mapping on simulated climate change signal: a case study over Central Italy, *Theor Appl Climatol*, 135, 725–740, <https://doi.org/10.1007/s00704-018-2406-8>, 2019.

- 690 Scaff, L., Prein, A. F., Li, Y., Liu, C., Rasmussen, R., and Ikeda, K.: Simulating the convective precipitation diurnal cycle in North America's current and future climate, *Clim Dyn*, 55, 369–382, <https://doi.org/10.1007/s00382-019-04754-9>, 2019.
- Sexton, D. M. H., McSweeney, C. F., Rostron, J. W., Yamazaki, K., Booth, B. B. B., Murphy, J. M., Regayre, L., Johnson, J. S., and Karmalkar, A. V.: A perturbed parameter ensemble of HadGEM3-GC3.05 coupled model projections: part 1: selecting the parameter combinations, *Clim Dyn*, 56, 3395–3436, <https://doi.org/10.1007/s00382-021-05709-9>, 2021.
- 695 Shah, M., Thakkar, A., and Shastri, H.: Comparative analysis of bias correction techniques for future climate assessment using CMIP6 hydrological variables for the Indian subcontinent, *Acta Geophys.*, 1–17, <https://doi.org/10.1007/s11600-024-01378-4>, 2024.
- Smith, B. A., Birkinshaw, S. J., Lewis, E., McGrady, E., and Sayers, P.: Physically-based modelling of UK river flows under climate change, *Frontiers in Water*, 6, <https://doi.org/10.3389/frwa.2024.1468855>, 2025.
- 700 Soares, P. M. M., Careto, J. A. M., Cardoso, R. M., Goergen, K., Katragkou, E., Sobolowski, S., Coppola, E., Ban, N., Belušić, D., Berthou, S., Caillaud, C., Dobler, A., Hodnebrog, Ø., Kartsios, S., Lenderink, G., Lorenz, T., Milovac, J., Feldmann, H., Pichelli, E., Truhetz, H., Demory, M. E., de Vries, H., Warrach-Sagi, K., Keuler, K., Raffa, M., Tölle, M., Sieck, K., and Bastin, S.: The added value of km-scale simulations to describe temperature over complex orography: the CORDEX FPS-Convection multi-model ensemble runs over the Alps, *Clim Dyn*, 62, 4491–4514, <https://doi.org/10.1007/s00382-022-06593-7>, 2024.
- 705 Tabari, H., Paz, S. M., Buekenhout, D., and Willems, P.: Comparison of statistical downscaling methods for climate change impact analysis on precipitation-driven drought, *Hydrology and Earth System Sciences*, 25, 3493–3517, <https://doi.org/10.5194/hess-25-3493-2021>, 2021.
- Tani, S. and Gobiet, A.: Quantile mapping for improving precipitation extremes from regional climate models, *Journal of Agrometeorology*, 21, 434–443, <https://doi.org/10.54386/jam.v21i4.278>, 2019.
- 710 Teutschbein, C. and Seibert, J.: Bias correction of regional climate model simulations for hydrological climate-change impact studies: Review and evaluation of different methods, *Journal of Hydrology*, 456–457, 12–29, <https://doi.org/10.1016/j.jhydrol.2012.05.052>, 2012.
- Themeßl, M. J., Gobiet, A., and Leuprecht, A.: Empirical-statistical downscaling and error correction of daily precipitation from regional climate models, *International Journal of Climatology*, 31, 1530–1544, <https://doi.org/10.1002/joc.2168>, 2011.
- 715 Themeßl, M. J., Gobiet, A., and Heinrich, G.: Empirical-statistical downscaling and error correction of regional climate models and its impact on the climate change signal, *Climatic Change*, 112, 449–468, <https://doi.org/10.1007/s10584-011-0224-4>, 2012.
- 720 Thrasher, B., Maurer, E. P., McKellar, C., and Duffy, P. B.: Technical Note: Bias correcting climate model simulated daily temperature extremes with quantile mapping, *Hydrology and Earth System Sciences*, 16, 3309–3314, <https://doi.org/10.5194/hess-16-3309-2012>, 2012.
- Trapp, R. J., Robinson, E. D., Baldwin, M. E., Diffenbaugh, N. S., and Schwedler, B. R. J.: Regional climate of hazardous convective weather through high-resolution dynamical downscaling, *Clim Dyn*, 37, 677–688, <https://doi.org/10.1007/s00382-010-0826-y>, 2011.
- 725 Vautard, R., Kadygrov, N., Iles, C., Boberg, F., Buonomo, E., Bülow, K., Coppola, E., Corre, L., van Meijgaard, E., Nogherotto, R., Sandstad, M., Schwingshackl, C., Somot, S., Aalbers, E., Christensen, O. B., Ciarlo, J. M., Demory, M.-E., Giorgi, F., Jacob, D., Jones, R. G., Keuler, K., Kjellström, E., Lenderink, G., Levavasseur, G., Nikulin, G., Sillmann, J.,

- Solidoro, C., Sørland, S. L., Steger, C., Teichmann, C., Warrach-Sagi, K., and Wulfmeyer, V.: Evaluation of the Large EURO-CORDEX Regional Climate Model Ensemble, *Journal of Geophysical Research: Atmospheres*, 126, e2019JD032344, <https://doi.org/10.1029/2019JD032344>, 2021.
- 730 Vichot-Llano, A., Martinez-Castro, D., Giorgi, F., Bezanilla-Morlot, A., and Centella-Artola, A.: Comparison of GCM and RCM simulated precipitation and temperature over Central America and the Caribbean, *Theor Appl Climatol*, 143, 389–402, <https://doi.org/10.1007/s00704-020-03400-3>, 2020.
- Weisman, M. L., Davis, C., Wang, W., Manning, K. W., and Klemp, J. B.: Experiences with 0–36-h Explicit Convective Forecasts with the WRF-ARW Model, *Wea. Forecasting*, 23, 407–437, <https://doi.org/10.1175/2007WAF2007005.1>, 2008.
- 735 Weusthoff, T., Ament, F., Arpagaus, M., and Rotach, M. W.: Assessing the Benefits of Convection-Permitting Models by Neighborhood Verification: Examples from MAP D-PHASE, *Mon. Wea. Rev.*, 138, 3418–3433, <https://doi.org/10.1175/2010MWR3380.1>, 2010.
- Wilcke, R. A. I., Mendlik, T., and Gobiet, A.: Multi-Variable Error Correction of Regional Climate Models, *Climatic Change*, 120, 871–887, <https://doi.org/10.1007/s10584-013-0845-x>, 2013.
- 740 Yun, Y., Liu, C., Luo, Y., Liang, X., Huang, L., Chen, F., and Rasmmusen, R.: Convection-permitting regional climate simulation of warm-season precipitation over Eastern China, *Clim Dyn*, 54, 1469–1489, <https://doi.org/10.1007/s00382-019-05070-y>, 2020.